

Multibody decays

Dr Eva Gersabeck
University of Manchester

Outline

- Model independent methods
 - The Energy test
 - Earth movers distance
 - T-odd moments
 - binned methods (Miranda method and co.)
 - Phase space integrated results
- Model dependent methods
- Things I can not cover
 - Input from multibody decays to γ

Covered in the talks of
Tim, Jonas and
Wolfgang

Introduction

- Multibody decays: final states are reached mainly through resonances
- Unique sensitivity to phases
- Excellent environment for CP violation and mixing: strong-phase differences varying across the Dalitz plot enhance the sensitivity

$$\mathcal{A}_{CP}(P \rightarrow f) \equiv \frac{|\bar{A}|^2 - |A|^2}{|\bar{A}|^2 + |A|^2} \propto \sum_{i,j} |A_i| |A_j| \sin(\delta_i - \delta_j) \sin(\phi_i - \phi_j)$$

- Tests of QCD (spectroscopy, amplitude models)
- Huge samples: a blessing and a curse

MODEL INDEPENDENT METHODS

Why go model independent?

- Fast discovery tools
- Binned or unbinned methods
- Can be used for direct and indirect CP violation tests
 - Will cover direct CP violation today
 - By design sensitive to local asymmetries rather than to global asymmetries

The Energy test

Energy test

- The Energy test uses a distance function ψ_{ij} to compute a T value
- T compares the average distance between pairs of events in the phase space

$$T = \sum_{i,j>1}^n \frac{\psi_{ij}}{n(n-1)} + \sum_{i,j>1}^{\bar{n}} \frac{\psi_{ij}}{\bar{n}(\bar{n}-1)} - \sum_{i,j}^{n,\bar{n}} \frac{\psi_{ij}}{n\bar{n}}$$

Average distance in
the first sample

Average distance in the
second sample

Average distance
between the two
samples

- The distance function

$$\psi(d_{ij}) = e^{-d_{ij}^2/2\delta}$$

- Phase space distance

$$d_{ij}^2 = \sum_{k=1}^D (x_{k,i} - x_{k,j})^2$$

- Our case

$$x_{k,i} = m_{k,i}^2$$

Optimising the sensitivity

- δ is a tunable distance parameter describing the effective phase-space radius where a local asymmetry is measured
- δ is analogous to the bin size in a binned approach
- It must be:
 - Larger than the resolution of d_{ij}
 - Small enough not to dilute local asymmetries
 - Optimised value from sensitivity studies

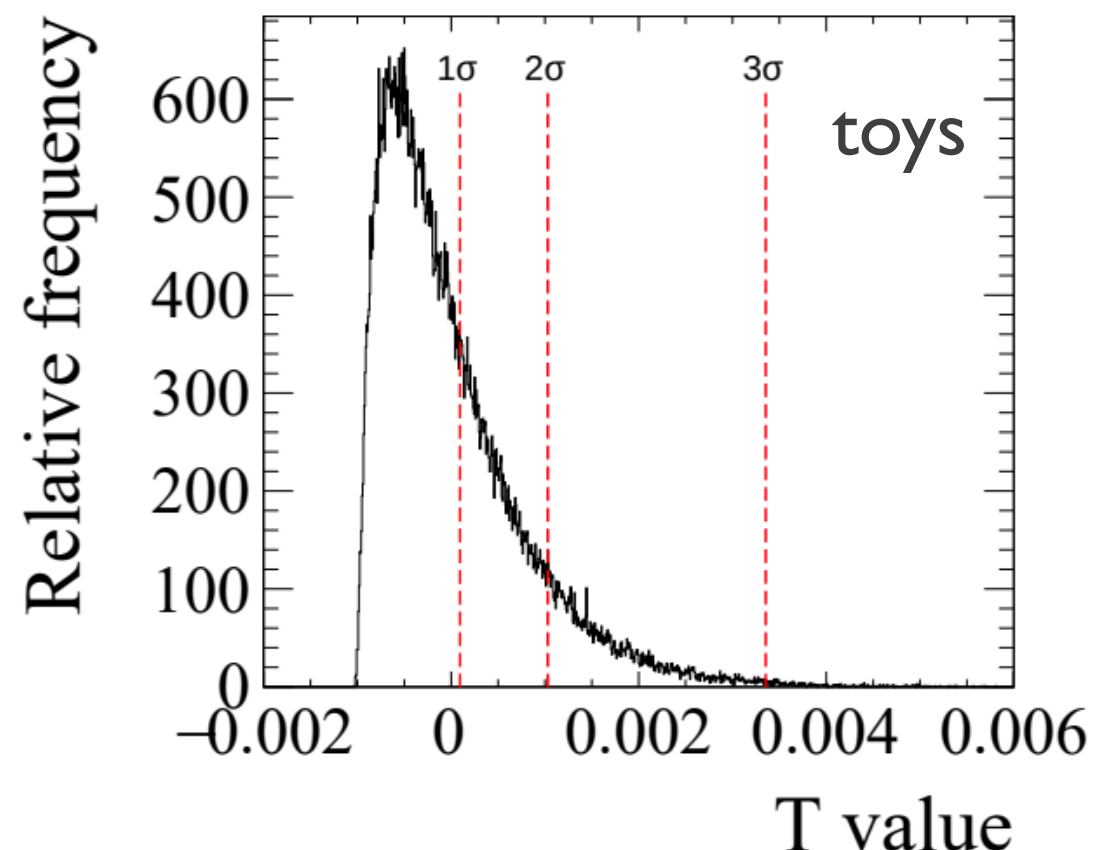
The Energy test in a nutshell

- Split sample is D^0 and \bar{D}^0 decays
- Compute reference T value
- Compute T values from permuted samples using random flavour tags (null hypothesis)
- Compute P-value = fraction of permuted T values $>$ reference T value

Used in: Phys. Rev. D102 (2020) 051101

Phys. Lett. B740 (2015) 158

Phys. Lett. B769 (2017) 345

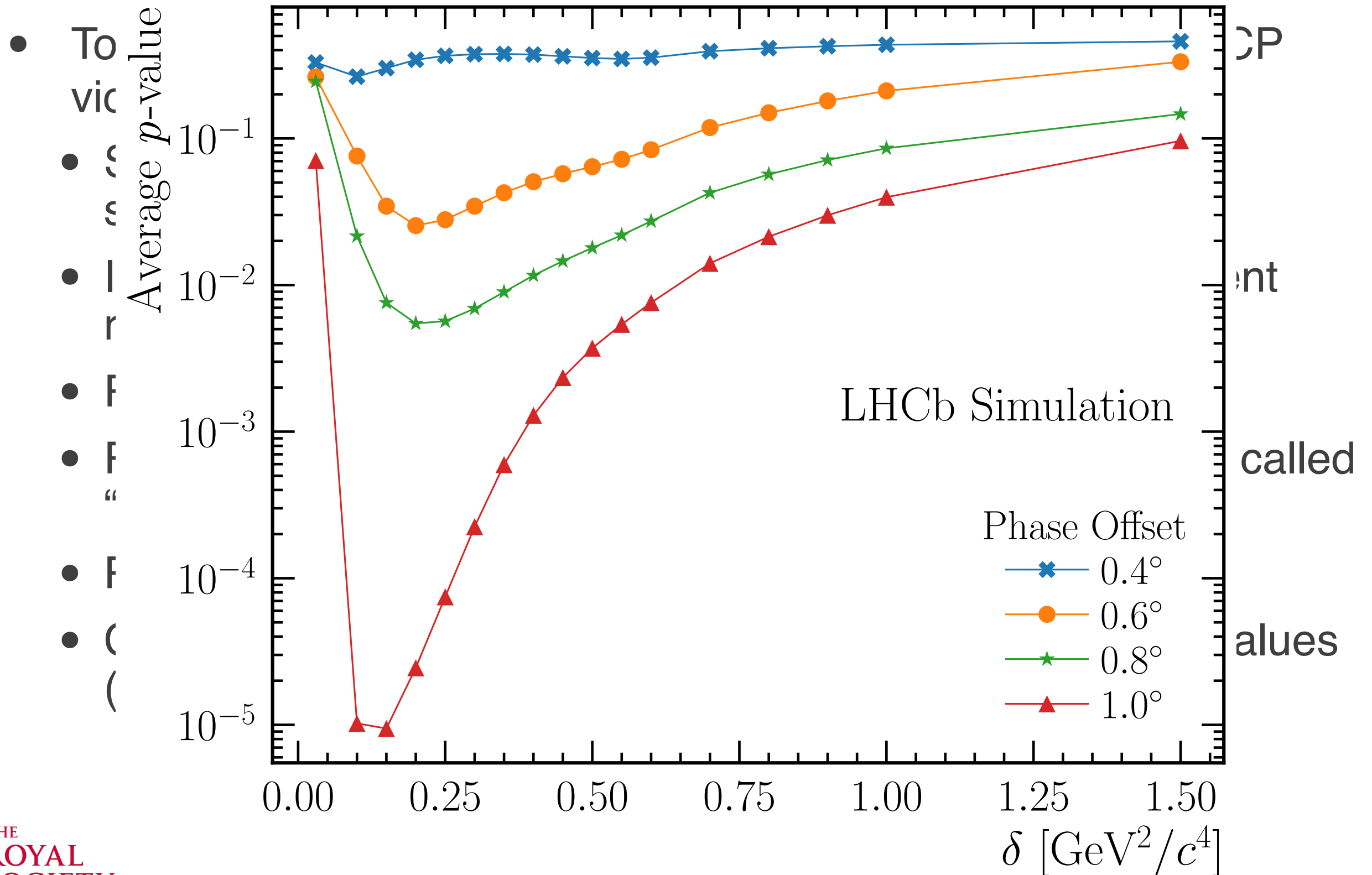


Sensitivity studies

- To verify that and how much the Energy test is sensitive to CP violation:
 - Simulate samples with comparable size to the Run 2 data samples
 - Input different amplitude and phase asymmetries in different resonances (e.g. 1%, 2%, 5%, 10% or $1^\circ, 2^\circ, 5^\circ, \dots$)
 - Run the Energy test
 - Reset and repeat for a set of δ values (i.e. perform a so called “ δ -scan”)
 - Plot the P-value distributions
 - Choose the δ value (or values) that ensures the lowest P-values (i.e. the best sensitivity)

Sensitivity studies

[arXiv:2306.12746]



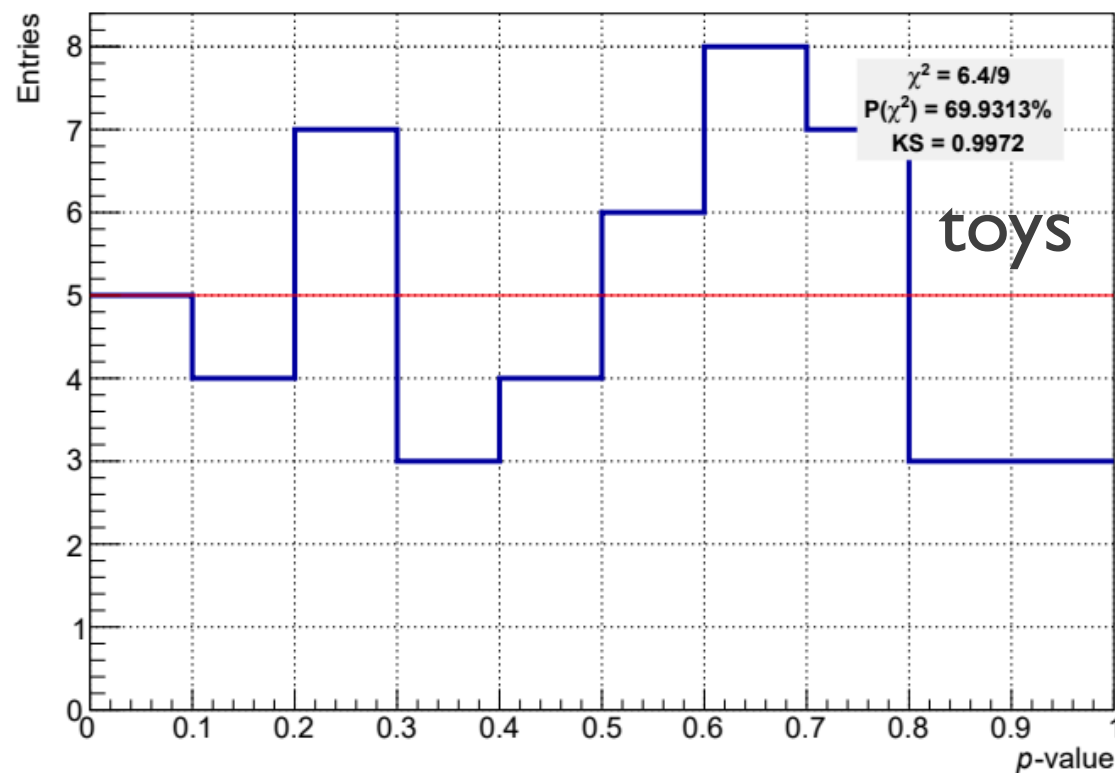
Validation of the Energy test

- To validate the Energy test is insensitive to instrumentation asymmetries a control channel is needed:
 - Same/ similar final state particles
 - No CP violation expected CF decays are great control samples
 - High statistics
- Apply signal requirement to control channels
 - Split into n subsamples with signal sample statistics
 - Run Energy test with optimised δ value
 - Compute and plot the P-values

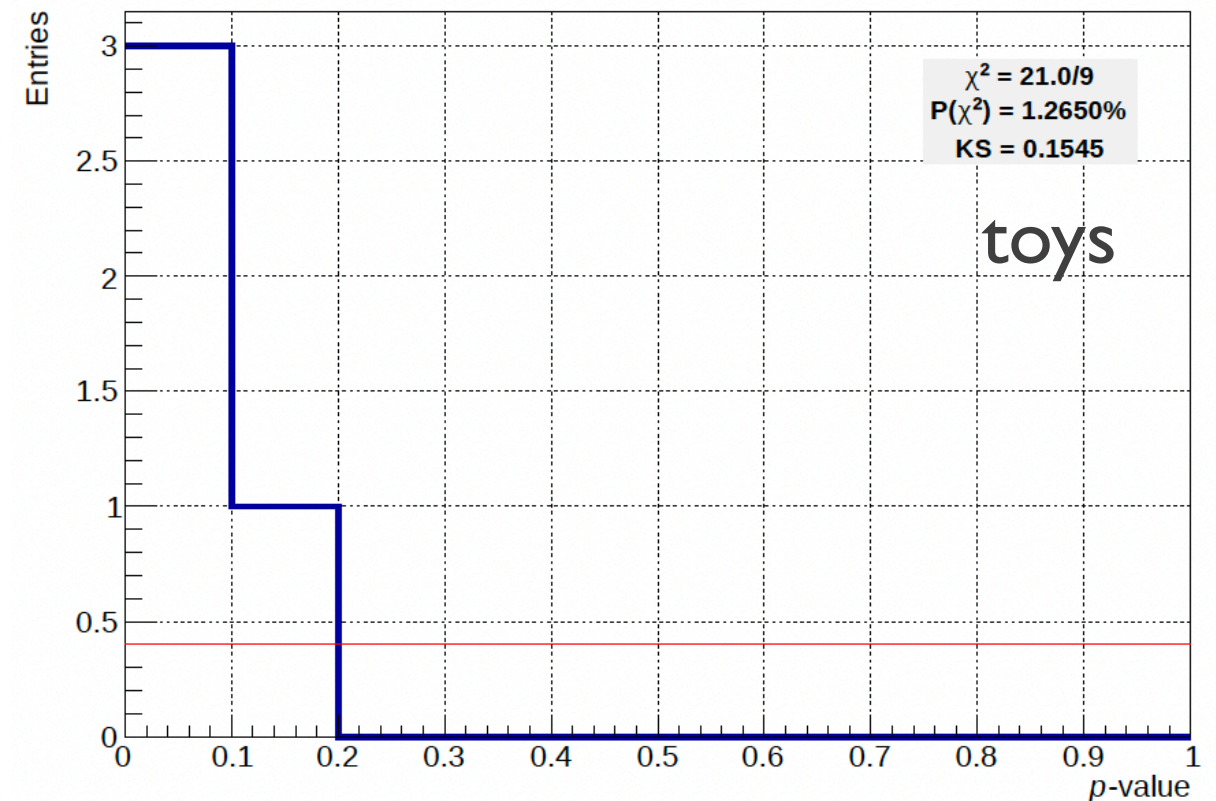
Symmetric or not?

- For visualisation only (toys):

My p -value distribution



Symmetric: flat distribution
of the p -values



Asymmetric: p -values
accumulate in the first bin

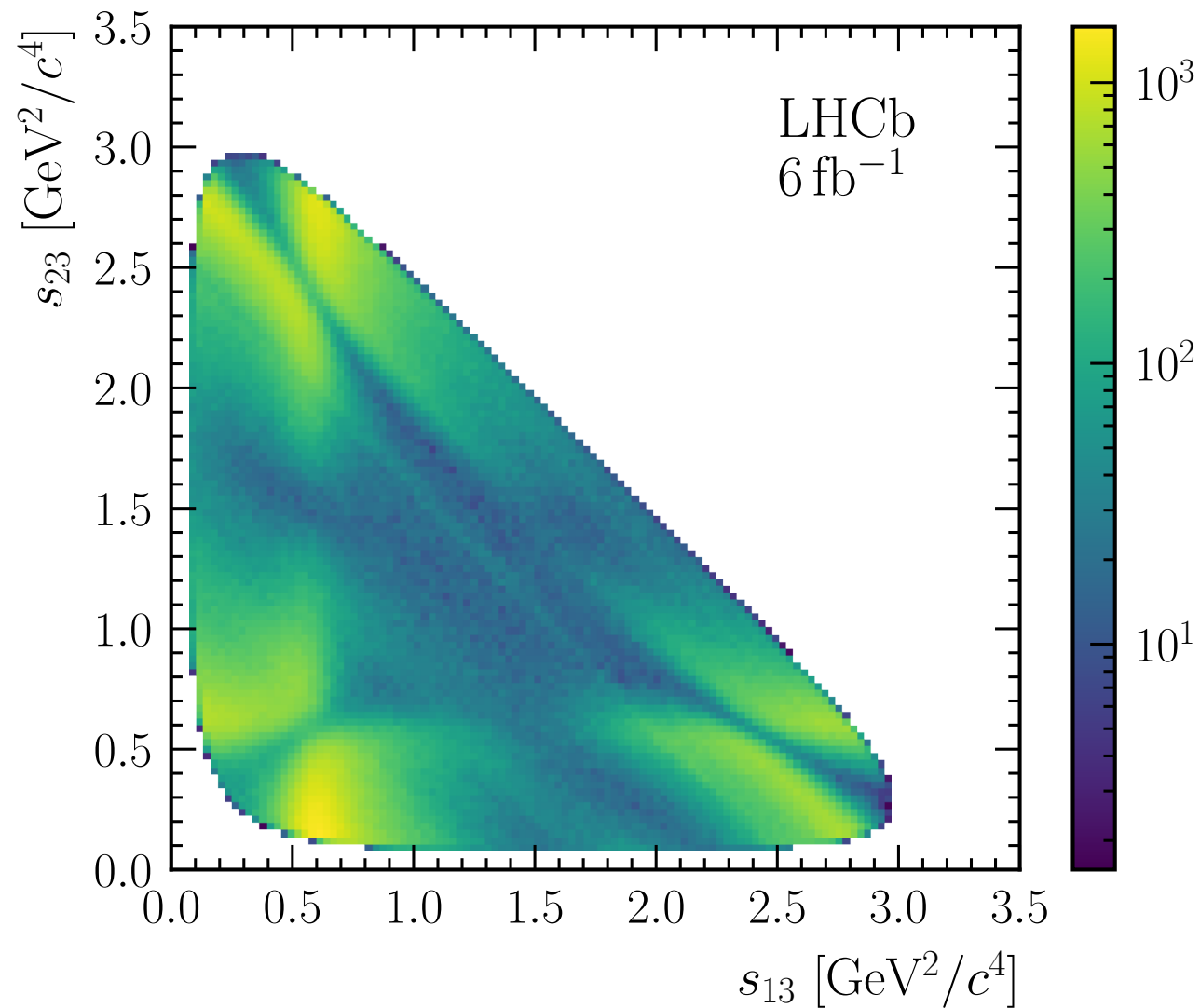
Search for CP violation in $D^0 \rightarrow \pi^+ \pi^- \pi^0$

[[arXiv:2306.12746](https://arxiv.org/abs/2306.12746)]

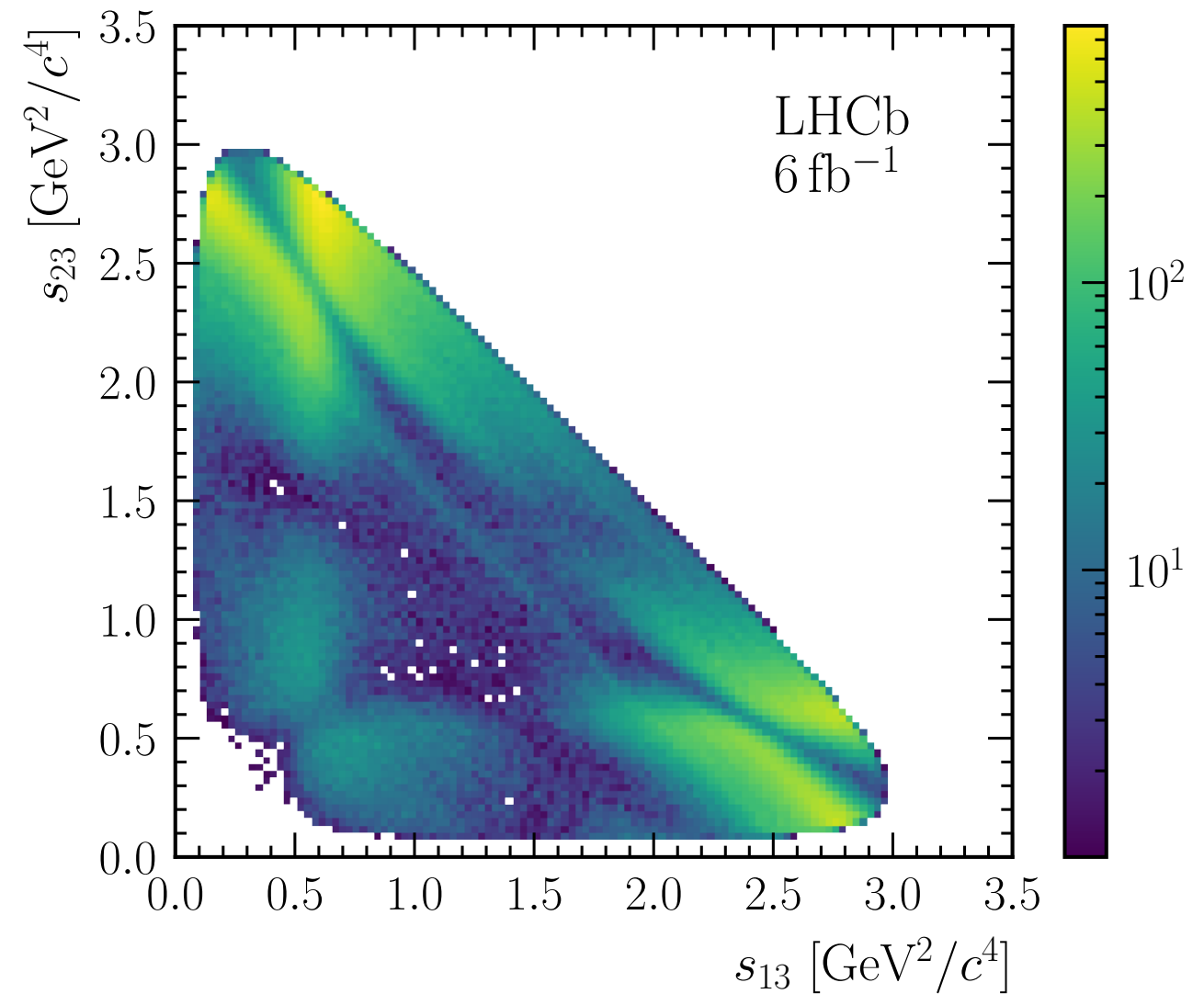
- Singly Cabibbo suppressed D^0 decays
- Prompt sample tagged by $D^{*+} \rightarrow D^0 \pi^+$
- Signal purity 81% for resolved π^0 and 91% for merged π^0
- LHCb Run 2 data (6 fb⁻¹)
- Four times larger than the Run 1 sample (PLB 2014 11 043)
- Control sample: $D^0 \rightarrow K^- \pi^+ \pi^0$
- Cross checks

Dalitz plot distributions

[arXiv:2306.12746]

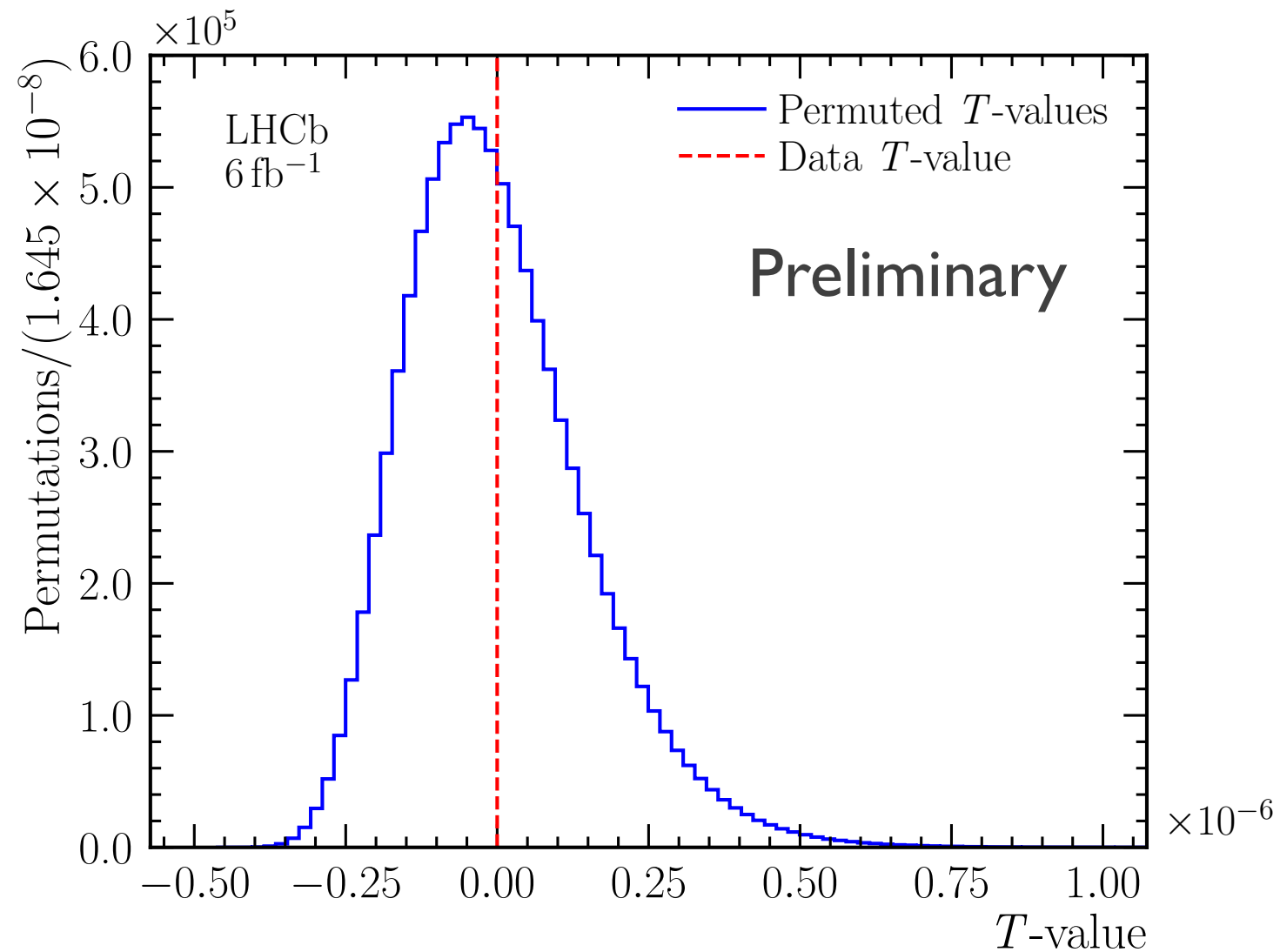


Resolved π⁰
1.7 M



Merged π⁰
0.8 M

- No evidence for local CP violation
- p-value = 61%



Earth movers distance

Earth mover's distance as a measure of CP violation

Adam Davis,^a Tony Menzo,^b Ahmed Youssef,^b Jure Zupan,^b

^aSchool of Physics and Astronomy, University of Manchester, M13 9PL, Manchester, UK

^bDepartment of Physics, University of Cincinnati, Cincinnati, Ohio 45221, USA

E-mail: adam.davis@manchester.ac.uk, menzoad@mail.uc.edu,
youssead@ucmail.uc.edu, zupanje@ucmail.uc.edu

ABSTRACT: We introduce a new unbinned two sample test statistic sensitive to CP violation utilizing the optimal transport plan associated with the Wasserstein (earth mover's) distance. The efficacy of the test statistic is shown via two examples of CP asymmetric distributions with varying sample sizes: the Dalitz distributions of $B^0 \rightarrow K^+\pi^-\pi^0$ and of $D^0 \rightarrow \pi^+\pi^-\pi^0$ decays. The windowed version of the Wasserstein distance test statistic is shown to have comparable sensitivity to CP violation as the commonly used energy test statistic, but also retains information about the localized distributions of CP asymmetry over the Dalitz plot. For large statistic datasets we introduce two modified Wasserstein distance based test statistics – the binned and the sliced Wasserstein distance statistics, which show comparable sensitivity to CP violation, but improved computing time and memory scalings. Finally, general extensions and applications of the introduced statistics are discussed.

distance metric
for EMD: $q=1$

$$W_q(\mathcal{E}, \bar{\mathcal{E}}) = \left[\min \sum_{i=1}^N \sum_{j=1}^{\bar{N}} f_{ij} (d_{ij})^q \right]^{1/q}$$

$$\sum_i^N f_{ij} = \frac{1}{\bar{N}}, \quad \sum_i^{\bar{N}} f_{ij} = \frac{1}{N}, \quad \sum_{i,j}^{N,\bar{N}} f_{ij} = 1$$

- The value of the EMD can be visualised as the work required to transport and reshape dirt (weighted samples) in the form of one distribution into the form of a second distribution.
- Toys for $B^0 \rightarrow K^+\pi^-\pi^0$ and $D^0 \rightarrow \pi^+\pi^-\pi^0$ generated with Laura++, no experimental results yet but looking forward

T-odd moments

T-odd moments method

Using triple product of final state particle momenta

$$C_T \equiv \vec{p}_1(\vec{p}_2 \times \vec{p}_3) \quad \bar{C}_T: \text{the triple product for the charge conjugate state}$$

Define triple product asymmetries

$$A_T \equiv \frac{\Gamma_{D^0}(C_T > 0) - \Gamma_{D^0}(C_T < 0)}{\Gamma_{D^0}(C_T > 0) + \Gamma_{D^0}(C_T < 0)}, \quad \bar{A}_T \equiv \frac{\Gamma_{\bar{D}^0}(-\bar{C}_T > 0) - \Gamma_{\bar{D}^0}(-\bar{C}_T < 0)}{\Gamma_{\bar{D}^0}(-\bar{C}_T > 0) + \Gamma_{\bar{D}^0}(-\bar{C}_T < 0)},$$

$$a_{CP}^{T\text{-odd}} \equiv \frac{1}{2}(A_T - \bar{A}_T) \quad a_P^{T\text{-odd}} \equiv \frac{1}{2}(A_T + \bar{A}_T)$$

Triple product asymmetries $\sim \sin\phi \cos\delta$

More careful consideration given in Durieux, Grossman
Phys. Rev. D 92, 076013 (2015)

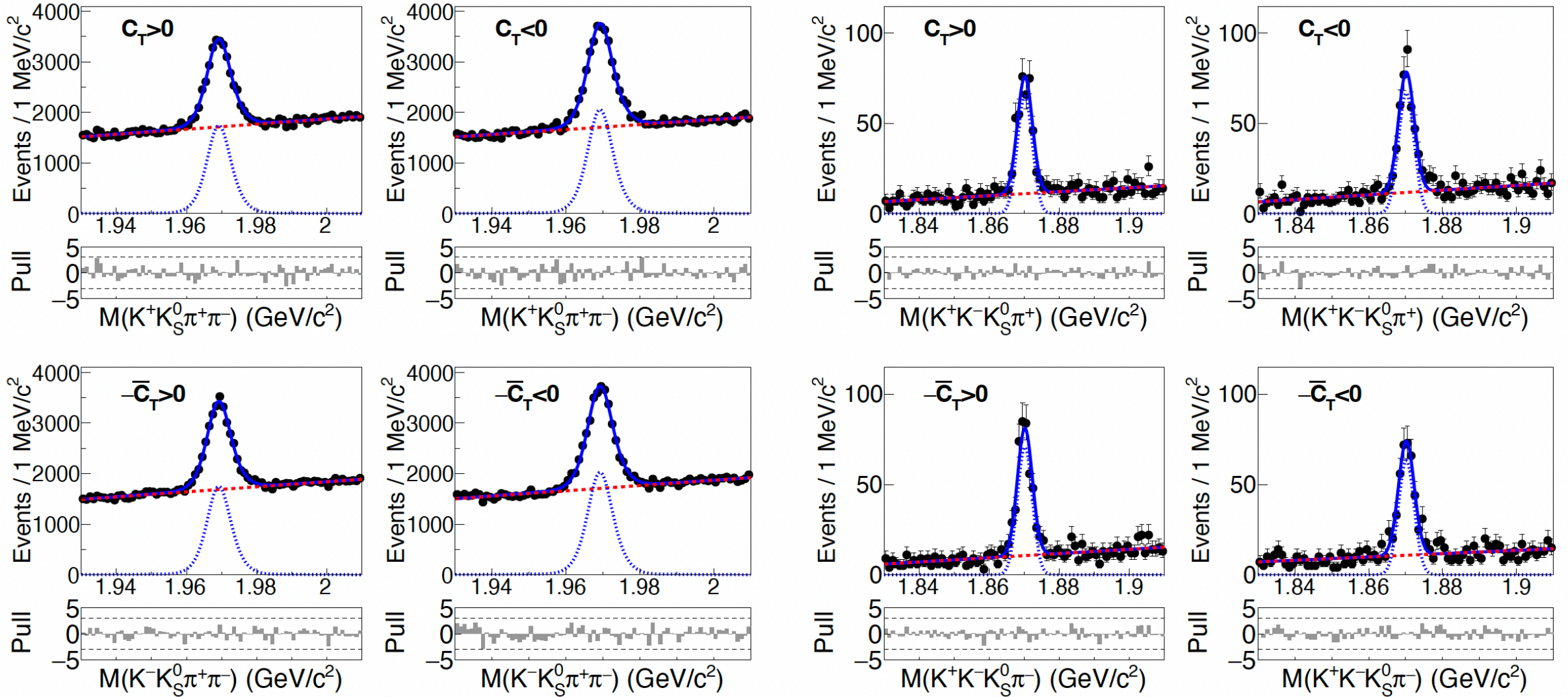
All production and detection effects cancel
T: reverses the momentum, similar to P
(no real time reversal)

Used in: BaBar: PRD 81 (2010) 111103
BaBar PRD 84, 031103 (R) (2011)
FOCUS: PLB 622 (2005) 239-248
LHCb: JHEP 1410 (2014) 005
LHCb: Phys. Rev. D 102 (2020) 051101

T-odd moments in $D^+_{(s)} \rightarrow K^+ K^0_S h^+ h^-$



arXiv:2305.11405v1



$$a_{CP}^{T\text{-odd}}(D^+ \rightarrow K^+ K^0_S \pi^+ \pi^-) = (0.34 \pm 0.87 \pm 0.32)\%$$

$$a_{CP}^{T\text{-odd}}(D^+_s \rightarrow K^+ K^0_S \pi^+ \pi^-) = (-0.46 \pm 0.63 \pm 0.38)\%$$

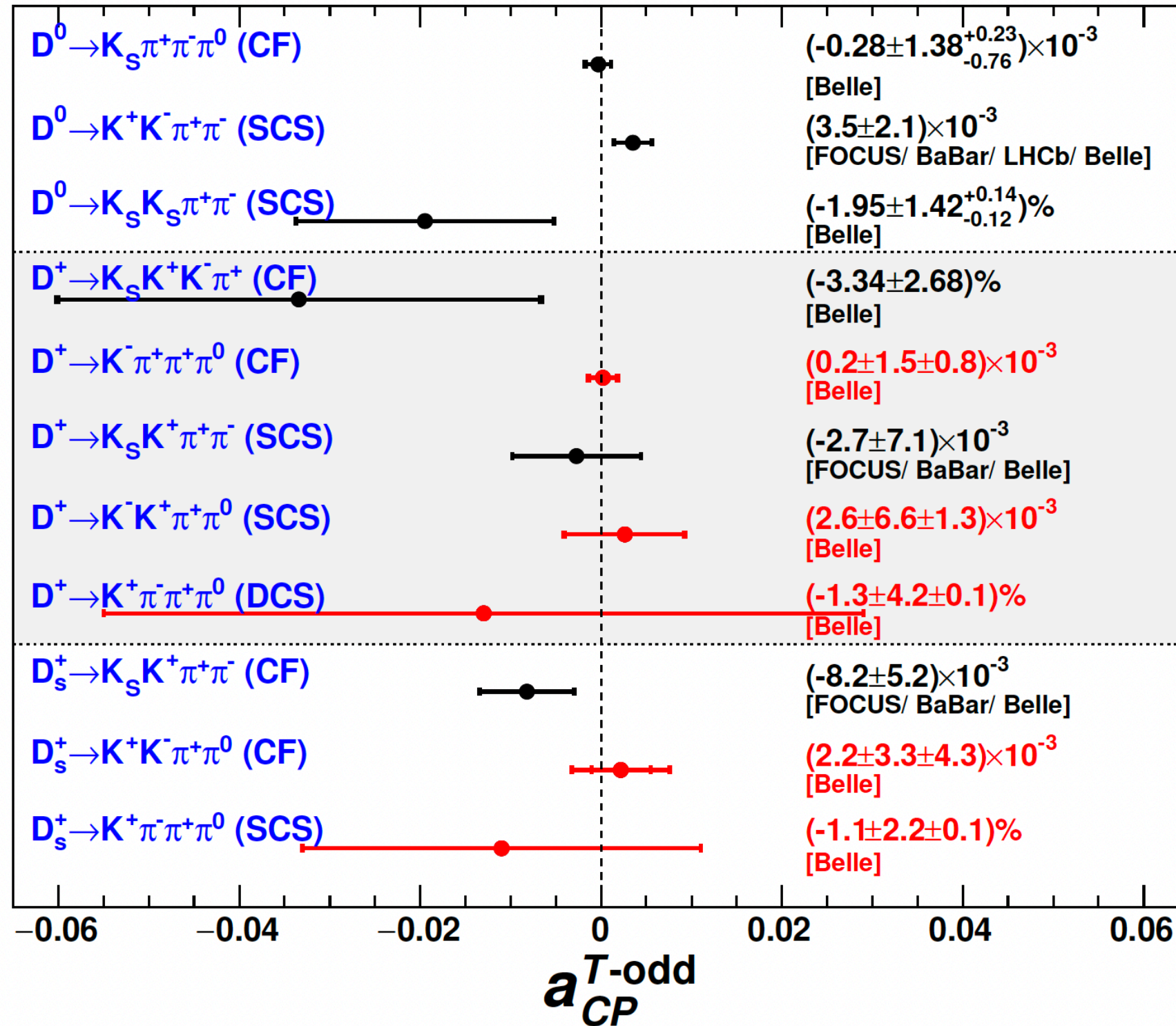
$$a_{CP}^{T\text{-odd}}(D^+ \rightarrow K^+ K^- K^0_S \pi^+) = (-3.34 \pm 2.66 \pm 0.35)\%,$$

T-odd moments in other $D^+_{(s)}$ modes



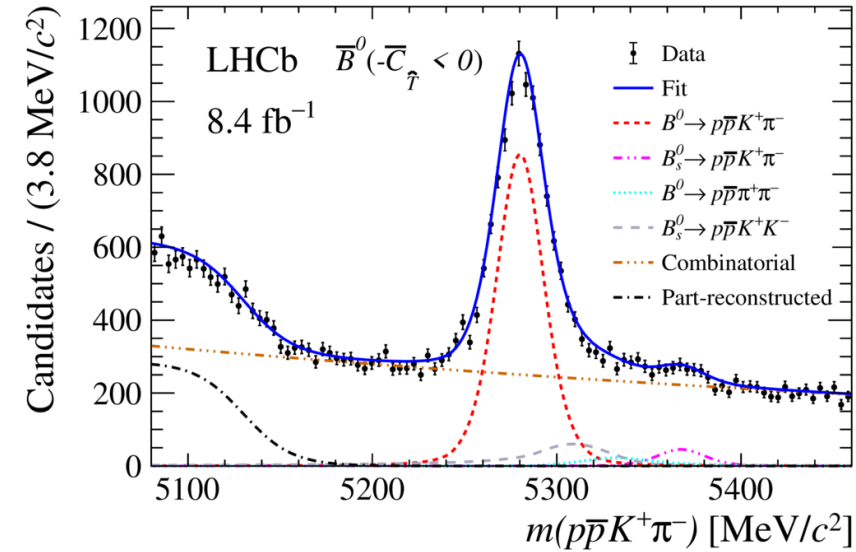
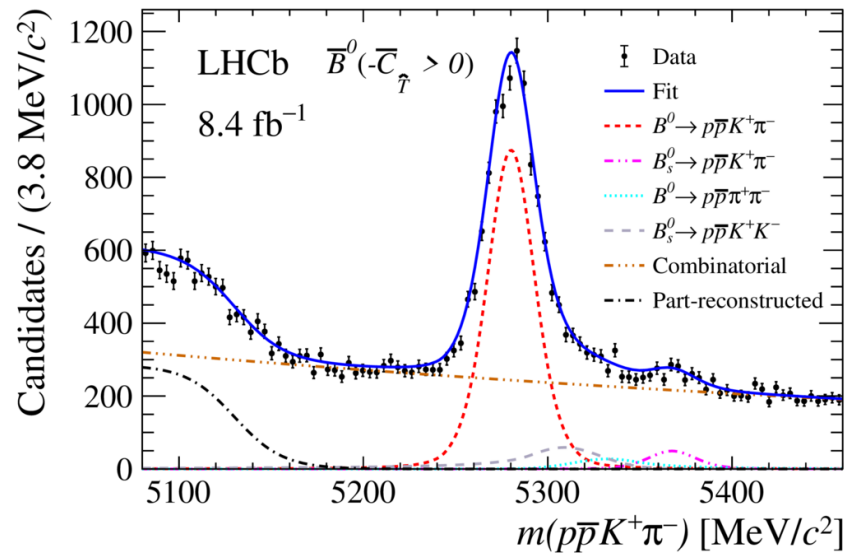
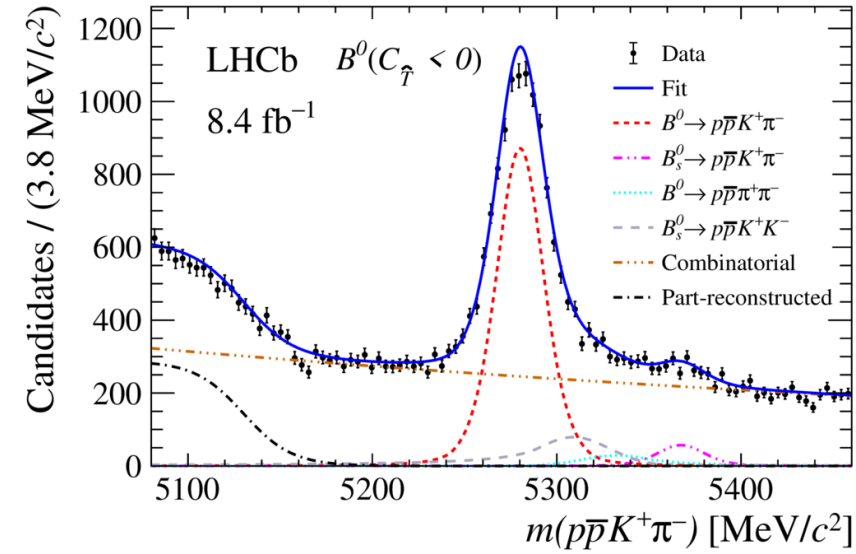
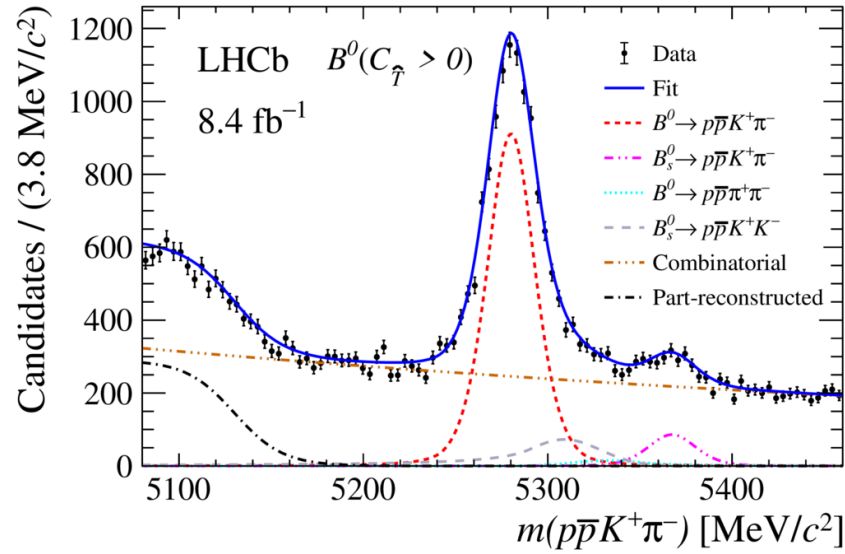
Recent measurements by Belle in red

arXiv:2305.12806v1



T-odd results $B^0 \rightarrow p\bar{p}K^+\pi^-$

arXiv:2205.08973v1

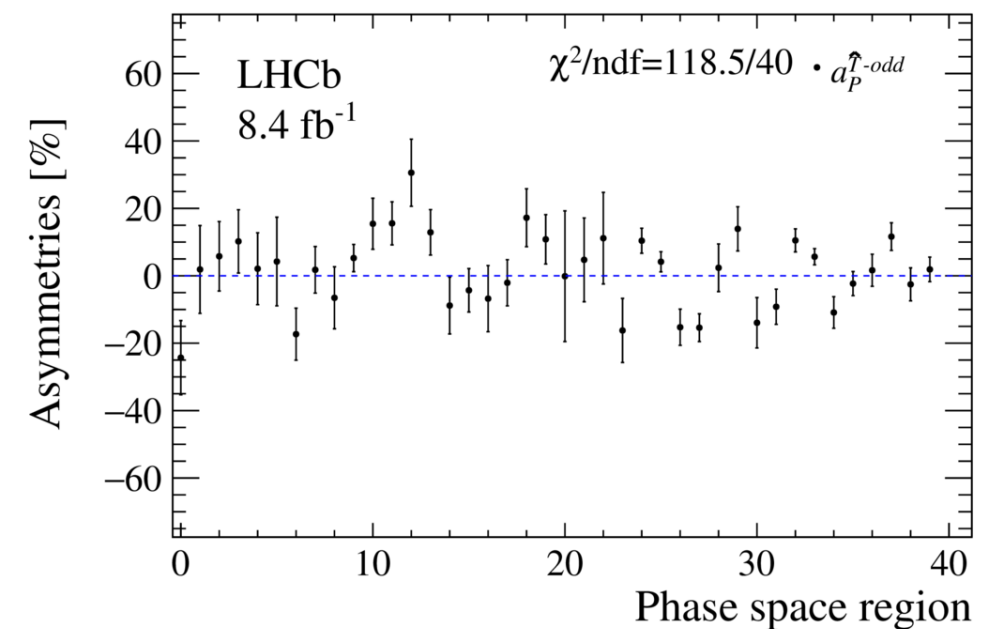
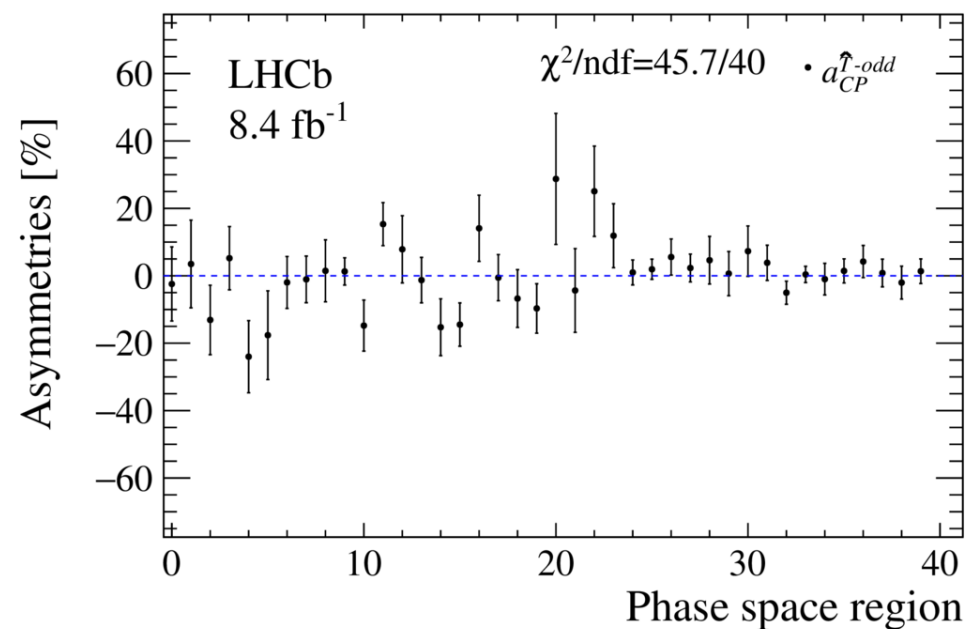
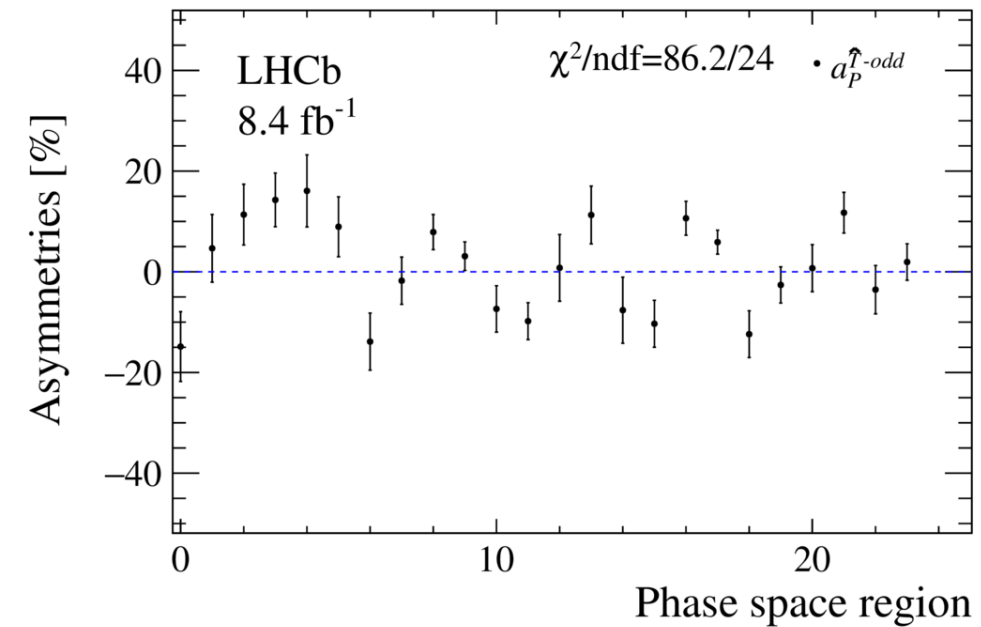
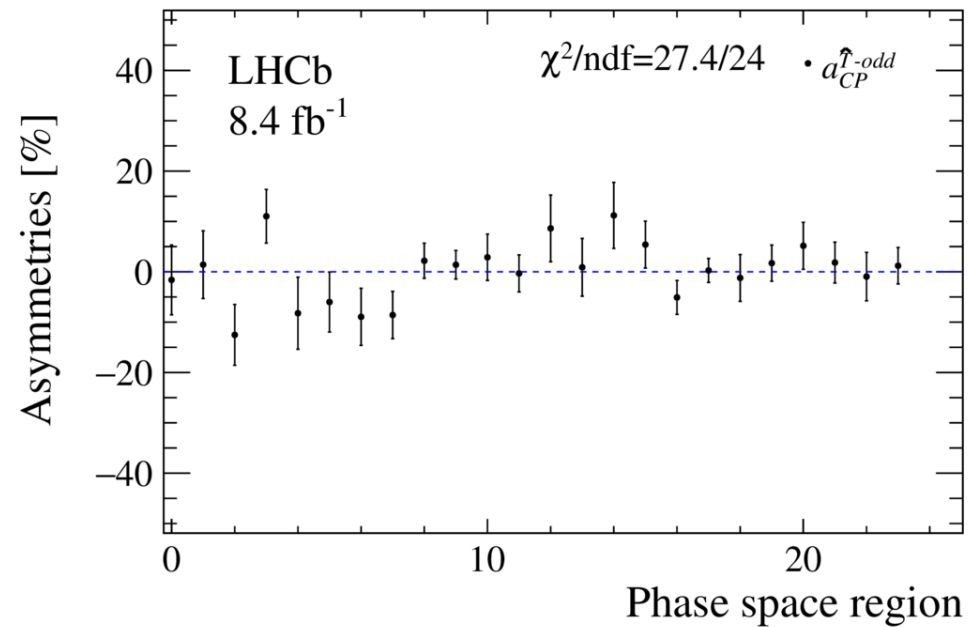


$$C_{\hat{T}} = \vec{p}_{K^+} \cdot (\vec{p}_{\pi^-} \times \vec{p}_p), \quad \bar{C}_{\hat{T}} = \vec{p}_{K^-} \cdot (\vec{p}_{\pi^+} \times \vec{p}_{\bar{p}}).$$

$$a_P^{T\text{-odd}} = (1.49 \pm 0.85 \pm 0.08)\%,$$

$$a_{CP}^{\hat{T}\text{-odd}} = (0.51 \pm 0.85 \pm 0.08)\%,$$

In phase space regions



No CP violation

Observed P violation: $\chi^2=86.2/24$ ($\chi^2=118.5/40$) translates to p-value of 6.1×10^{-9} (1.1×10^{-9}), corresponding to 5.8σ (6.0σ) deviation

Comparing binned Dalitz plots

The Miranda method

Introduced by BaBar: PRD78, 051102 (2008). Developed further in PRD 80, 096006 (2009), PRD86, 036005 (2012)

- Divide the Dalitz plot in two-dimensional bins
- Compute, for each bin, the significance of the difference in the numbers of $D^+_{(s)}$ candidates and $D^-_{(s)}$ candidates, where the latter is corrected for global charge asymmetry (e.g. from production and detection).

$$S_{CP}^i = \frac{N^i(D^+_{(s)}) - \alpha N^i(D^-_{(s)})}{\sqrt{\alpha(\delta_{N^i(D^+_{(s)})}^2) + \delta_{N^i(D^-_{(s)})}^2}}$$

$$\alpha = \frac{\sum_i N^i(D^+_{(s)})}{\sum_i N^i(D^-_{(s)})}$$

- Two-sample χ^2 test: calculate p-value for no-CPV hypothesis based on $\chi^2(\mathcal{S}_{CP}) = \sum (\mathcal{S}_{CP})^2$

Applied also to:

LHCb $D \rightarrow KK\pi$ PRD 84.112008 (2011)

LHCb $D \rightarrow 3\pi$ PLB 728 (2014) 585-595

CDF $D \rightarrow KS\pi\pi$ PRD 86, 032007 (2012)

LHCb $D \rightarrow \varphi\pi, D \rightarrow KS\pi$ JHEP 1306 (2013) 112

BaBar $D \rightarrow KK\pi$: PRD 87 (2013) 052010 (check)

LHCb $D^0 \rightarrow \pi\pi\pi\pi^0$ PLB 740, 158 (2015).

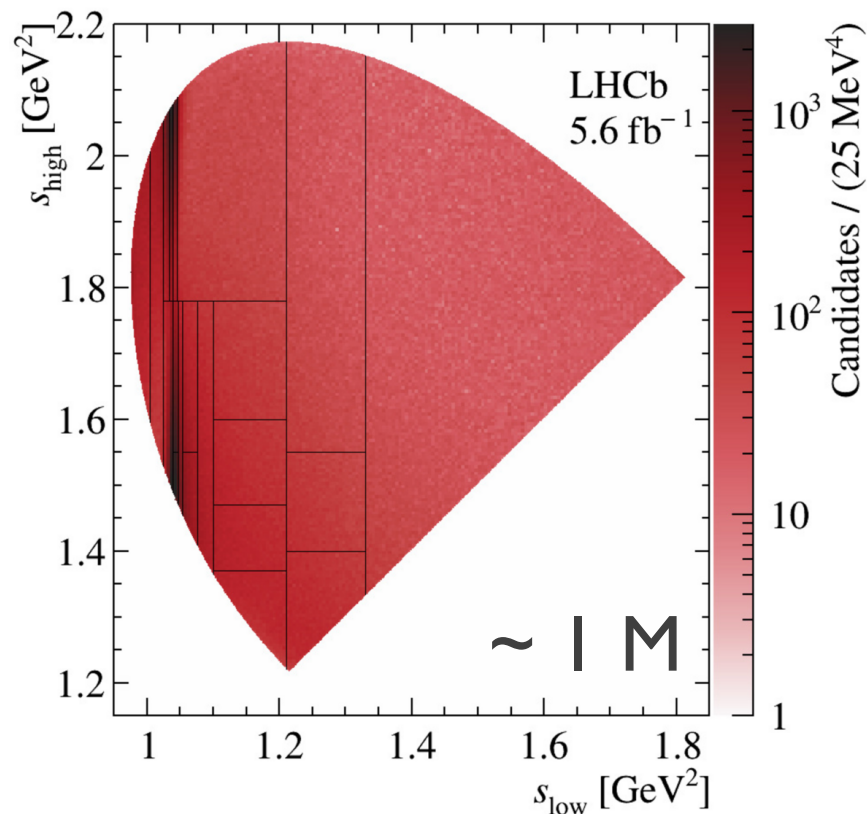
LHCb $D \rightarrow KK\pi\pi, D \rightarrow 4\pi$ PLB 726 (2013) 623-633 (5D bins)

Search for CP violation in $D^+_{(s)} \rightarrow K^-K^+K^+$

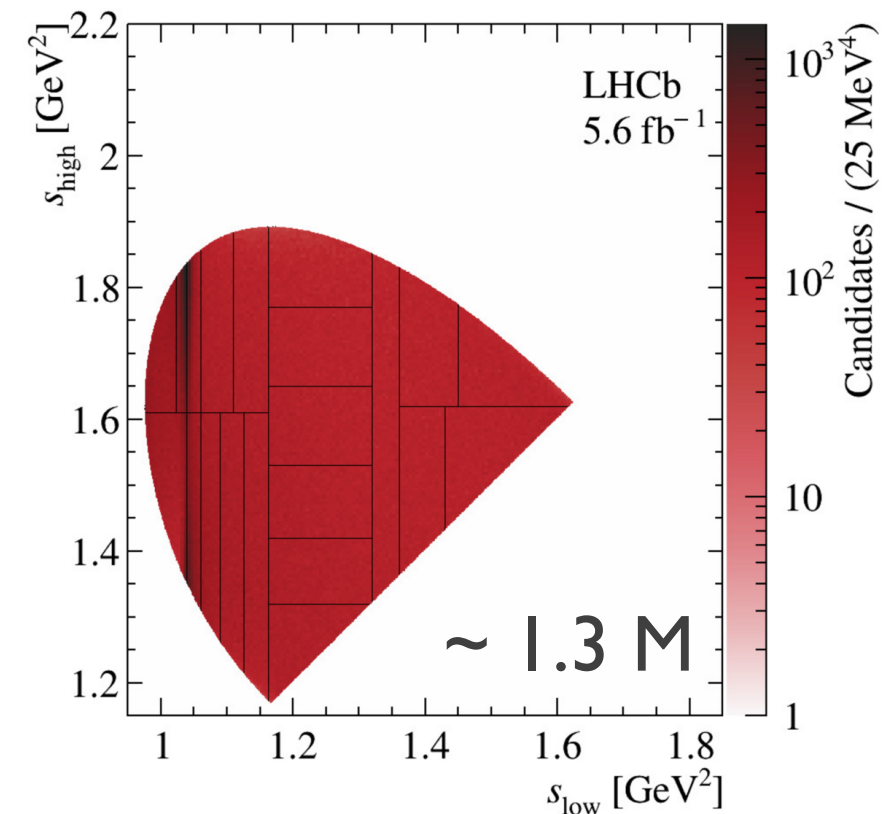
- Singly Cabibbo suppressed $D^+_{(s)}$ decays
- Signal purity 64% (D^+_s) and 78% (D^+)
- LHCb Run 2 data (5.6 fb^{-1})

21 bins in total overlaid

$D^+_s \rightarrow K^-K^+K^+$



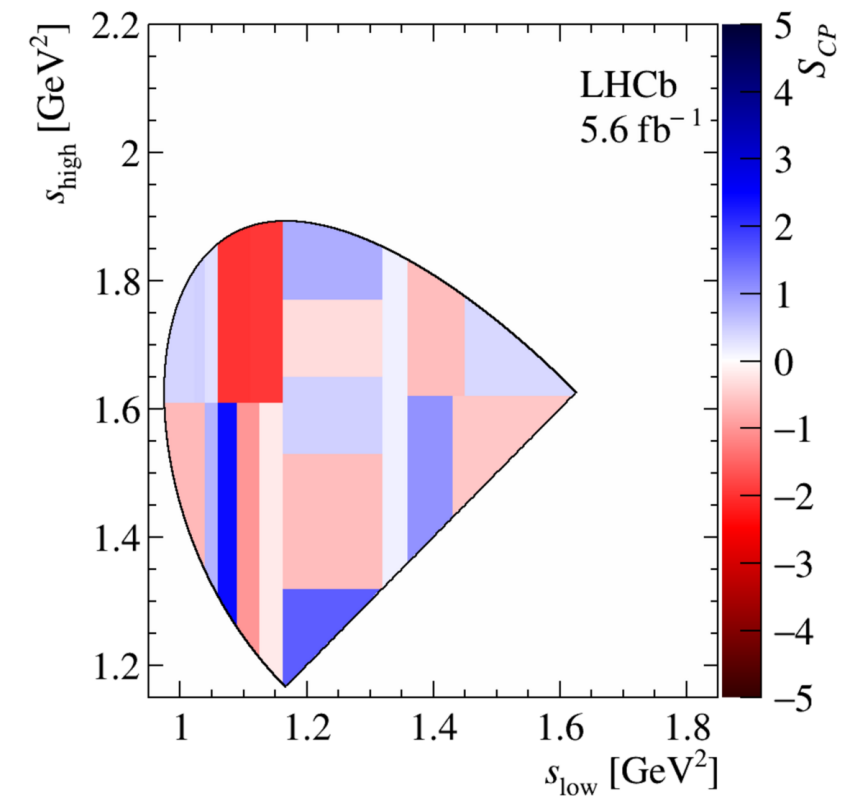
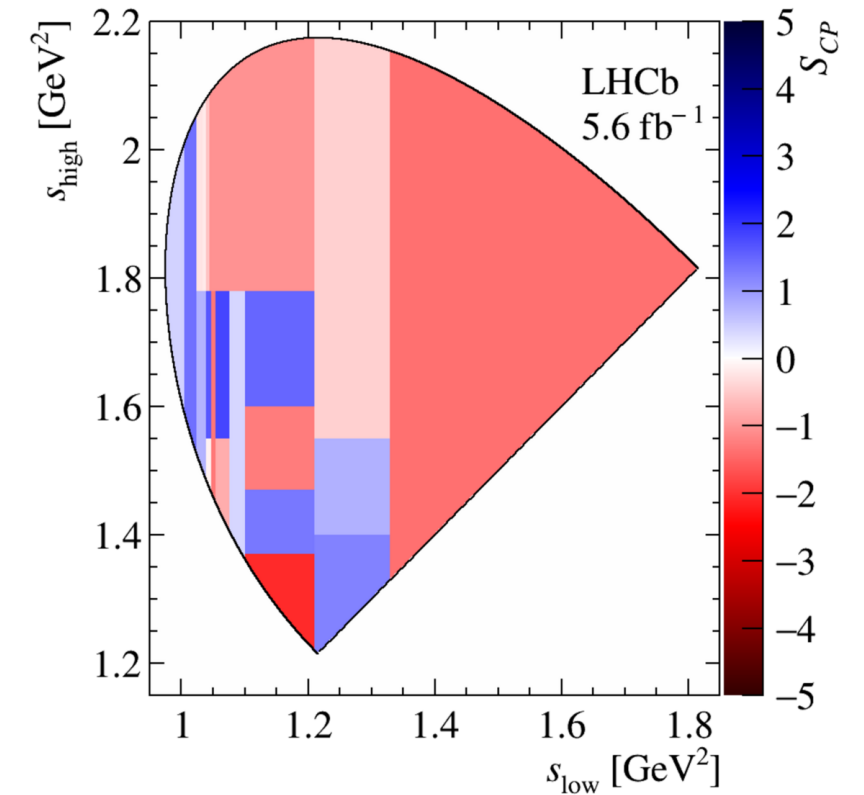
$D^+ \rightarrow K^-K^+K^+$



Modified Miranda: Fit in each bin, no background (fit per bin)

Results

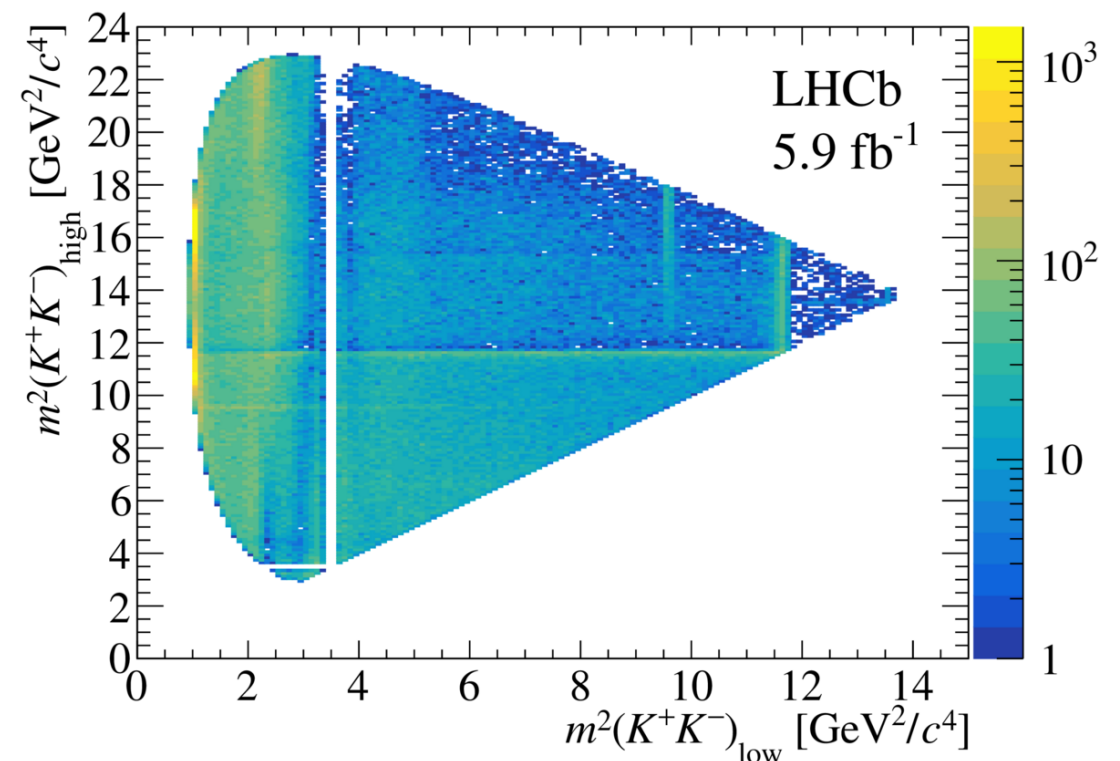
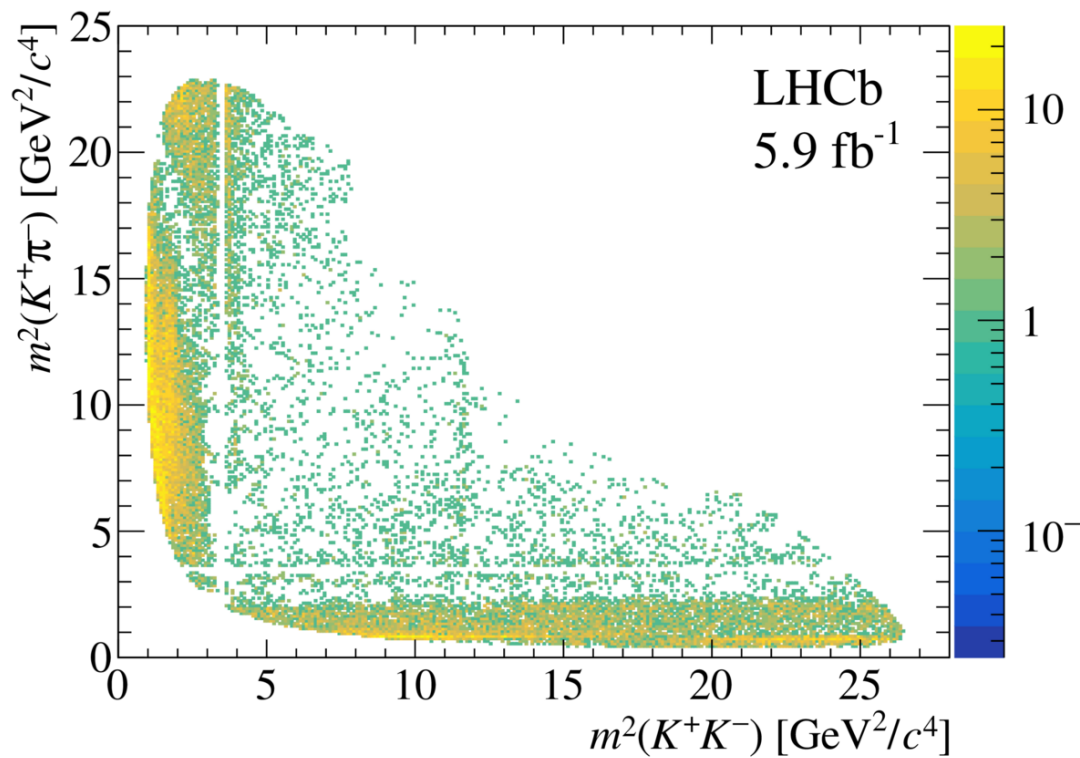
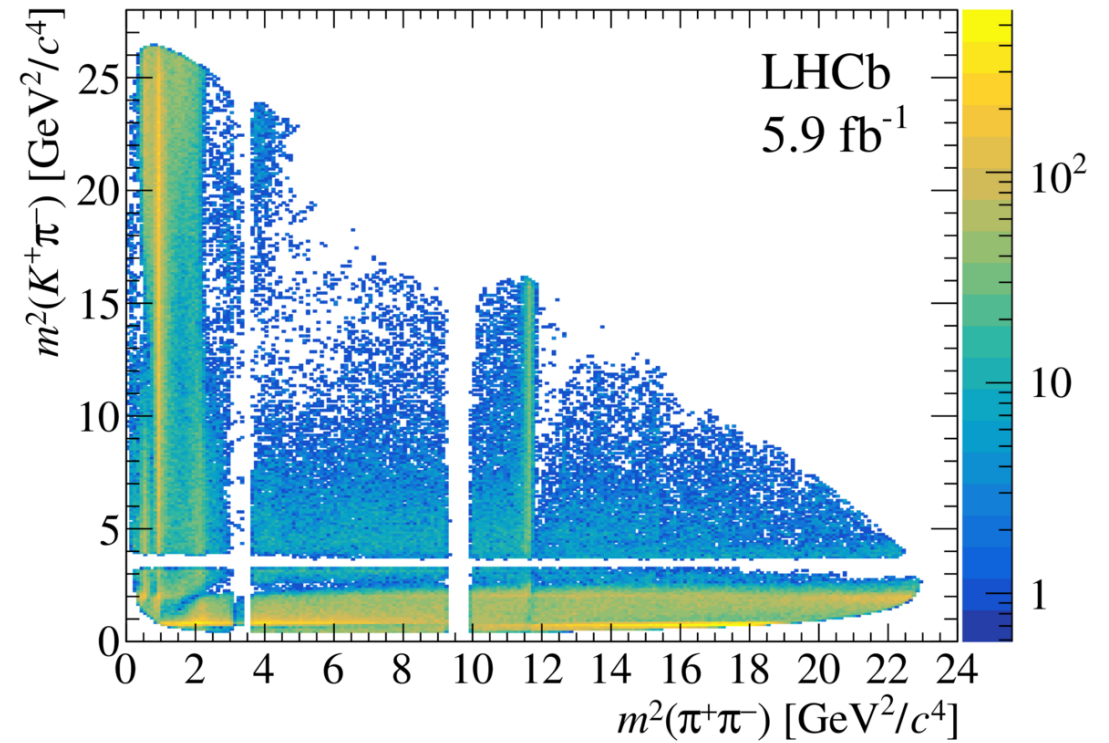
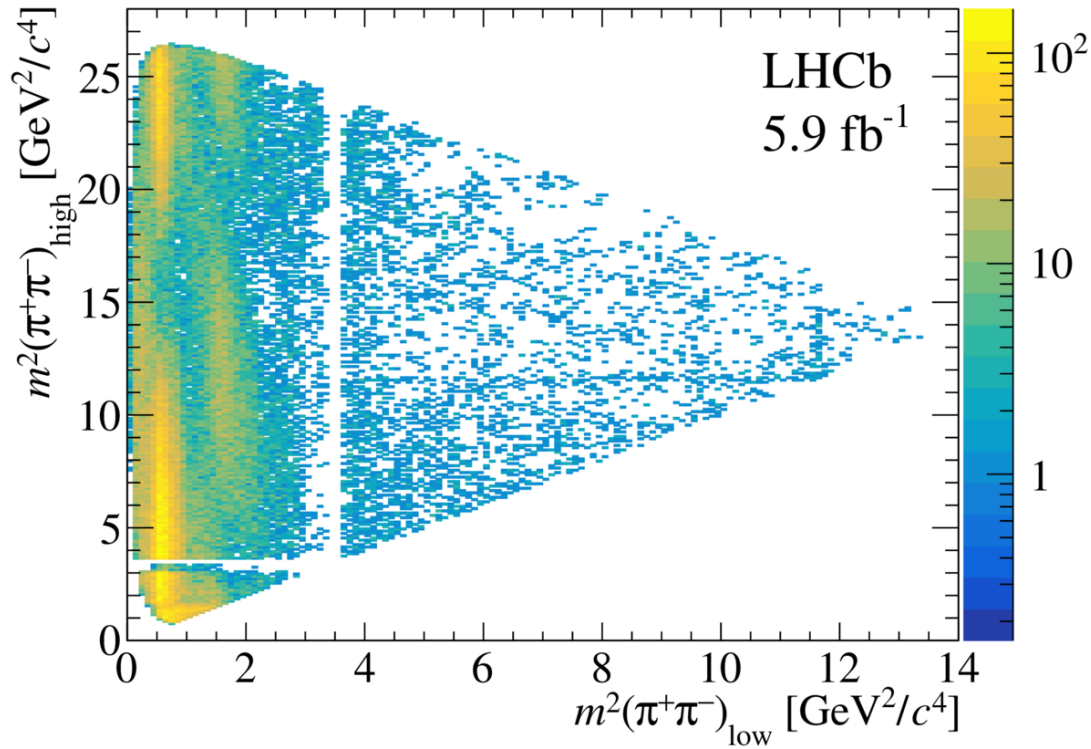
- Control samples:
 - Phase space simulation
 - Background samples
 - $D^+_s \rightarrow K^-K^+\pi^+$ and $D^+ \rightarrow K^-\pi^+\pi^+$ (CF)
- Stability checks:
 - different invariant mass fit models
 - different binning schemes
- No evidence for CP violation
 - p-value ($D^+_s \rightarrow K^-K^+K^+$) = 13.3%
 - p-value ($D^+ \rightarrow K^-K^+K^+$) = 31.6%



CP violation in $B^\pm \rightarrow hhh$

- Quite complex
- Short- and long-distance contributions to the generation of the strong-phase differences
- A recent amplitude analysis found a large CP asymmetry related to the **interference between the S- and P-wave contributions** in $B^+ \rightarrow \pi^+ \pi^+ \pi^-$ decays, **also in S- wave and in D- wave** [Phys. Rev. D101, (2020) 012006; Phys. Rev. Lett. 124, (2020) 031801]
- CP violation involving $\pi\pi \rightarrow KK$ rescattering was observed in $B^+ \rightarrow \pi^+ K^+ K^-$ decays : **$A_{CP} = (-66.4 \pm 3.8 \text{ (stat)} \pm 1.9 \text{ (syst)})\%$** [Phys. Rev. Lett. 123, (2019) 231802]
- The patterns of localised CP asymmetries in the four charmless decay modes $B^+ \rightarrow \pi^+ \pi^+ \pi^-$, $B^+ \rightarrow K^+ K^+ K^-$, $B^+ \rightarrow \pi^+ K^+ K^-$ and $B^+ \rightarrow K^+ \pi^+ \pi^-$ can be interpreted as originating from long-distance hadronic interactions

Phase space distributions



Binned asymmetries

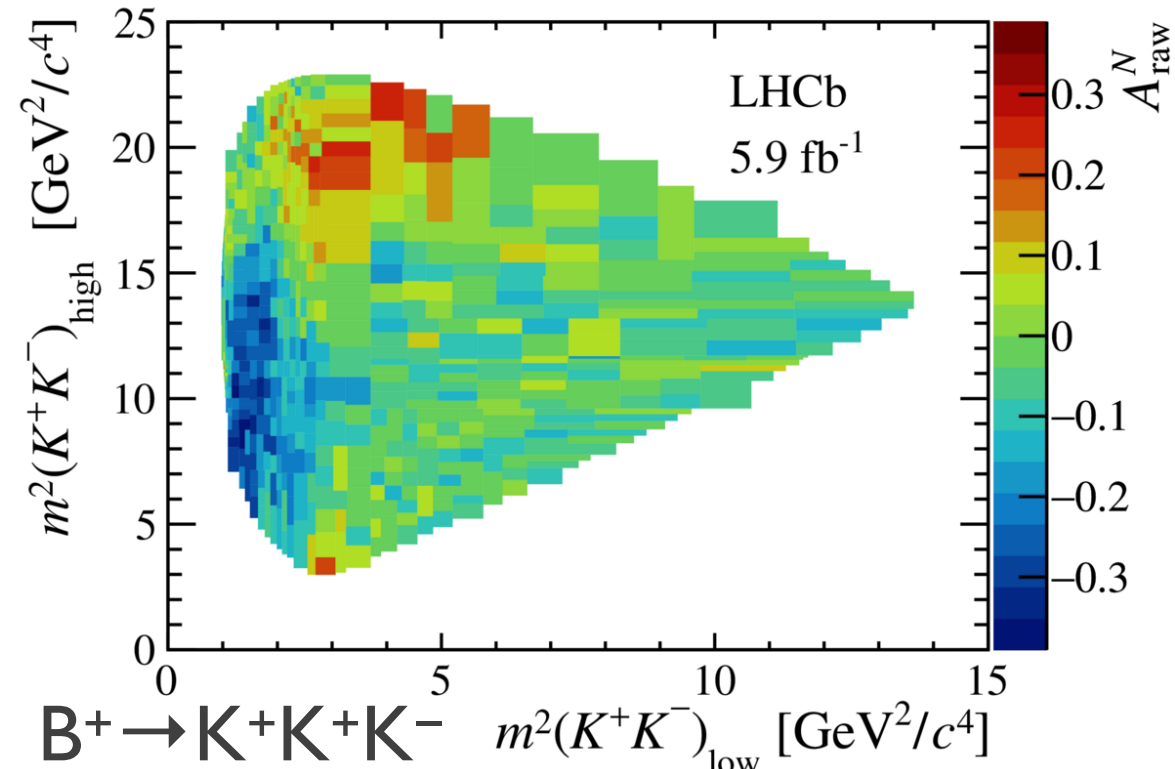
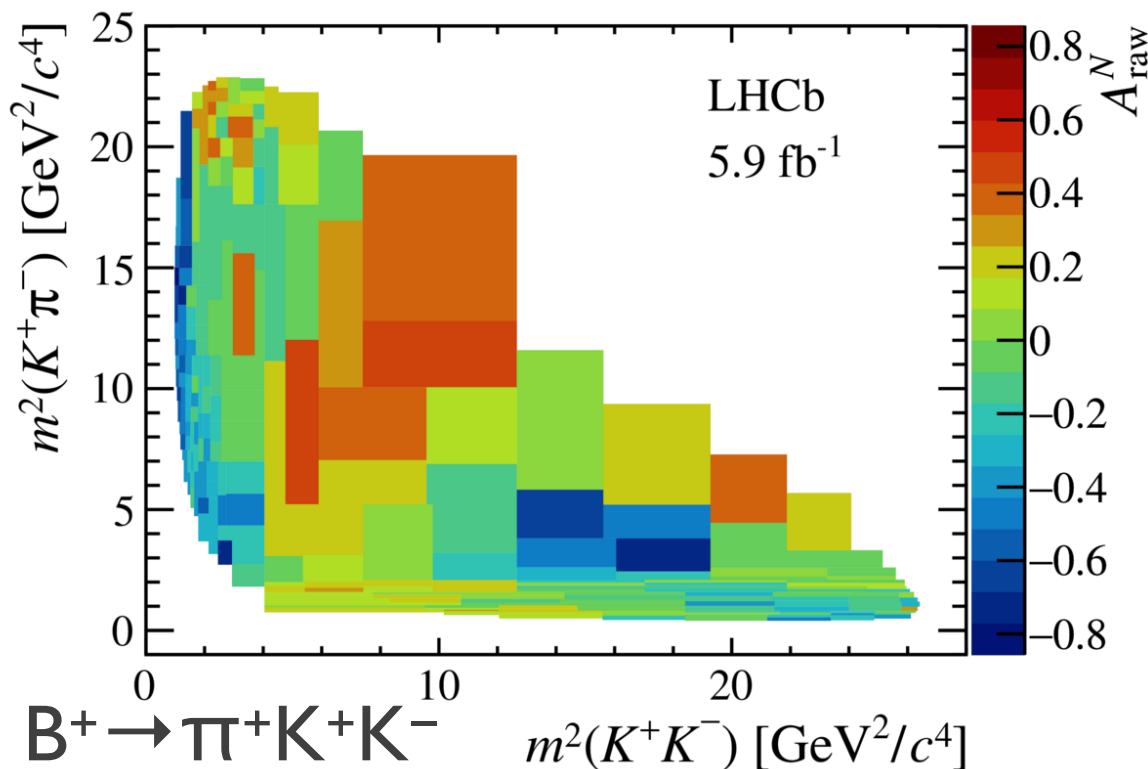
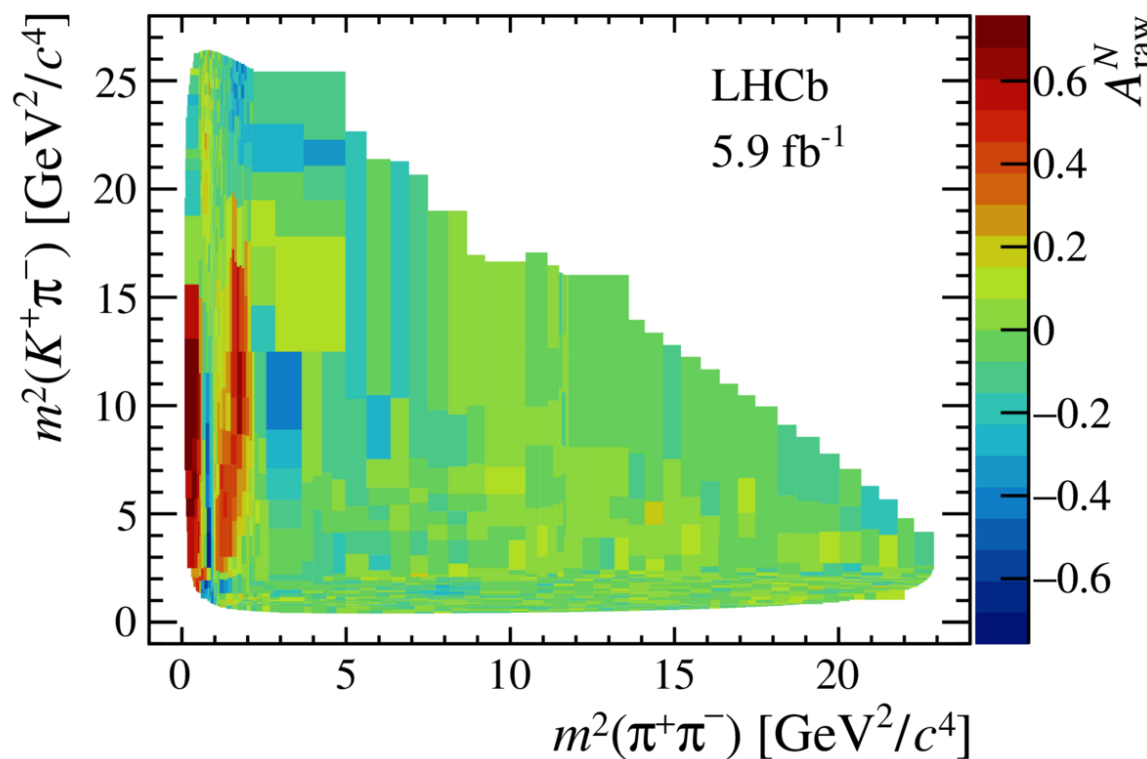
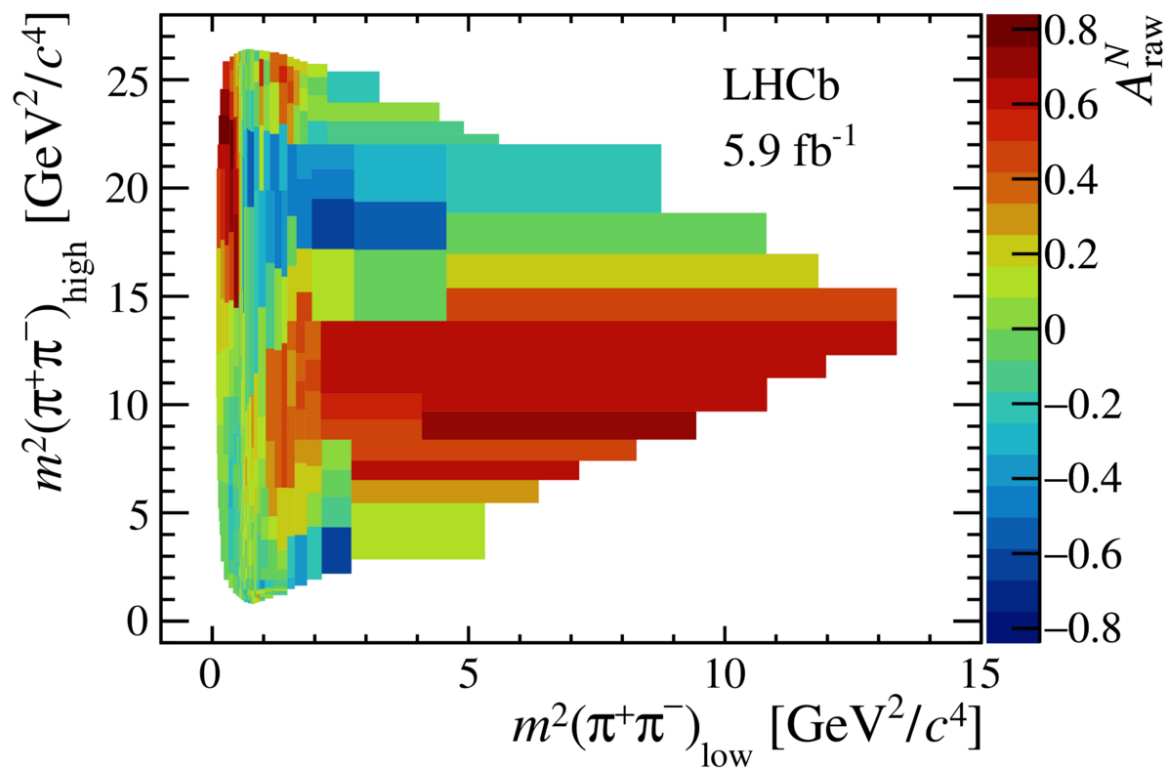
- Split by flavour
- Subtract the background, correct for efficiencies
- Calculate asymmetries per bin

$$A_{CP}(s_{12}, s_{23}) = \left(\frac{d\Gamma(\bar{P} \rightarrow \bar{f})}{d\Omega} - \frac{d\Gamma(P \rightarrow f)}{d\Omega} \right) / \left(\frac{d\Gamma(\bar{P} \rightarrow \bar{f})}{d\Omega} + \frac{d\Gamma(P \rightarrow f)}{d\Omega} \right)$$

- Adaptive binning: with approximately the same number of events
 - $B^\pm \rightarrow \pi^\pm \pi^+ \pi^-$: 400 bins \sim 229 events/bin
 - $B^\pm \rightarrow K^\pm \pi^+ \pi^-$: 1728 bins \sim 276 events/bin
 - $B^\pm \rightarrow \pi^\pm K^+ K^-$: 256 bins \sim 127 events/bin
 - $B^\pm \rightarrow K^\pm K^+ K^-$: 729 bins \sim 461 events/bin

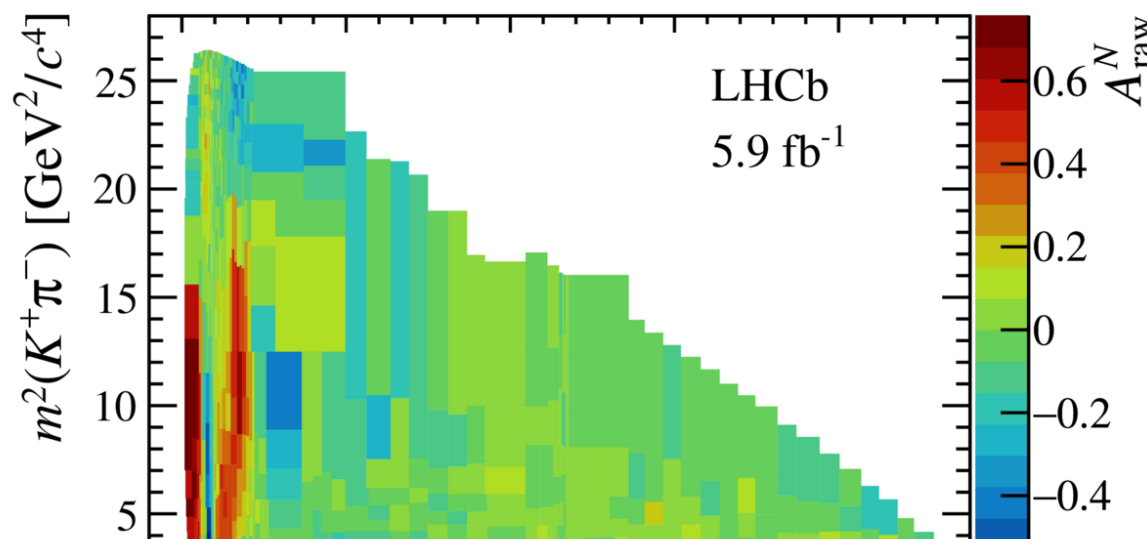
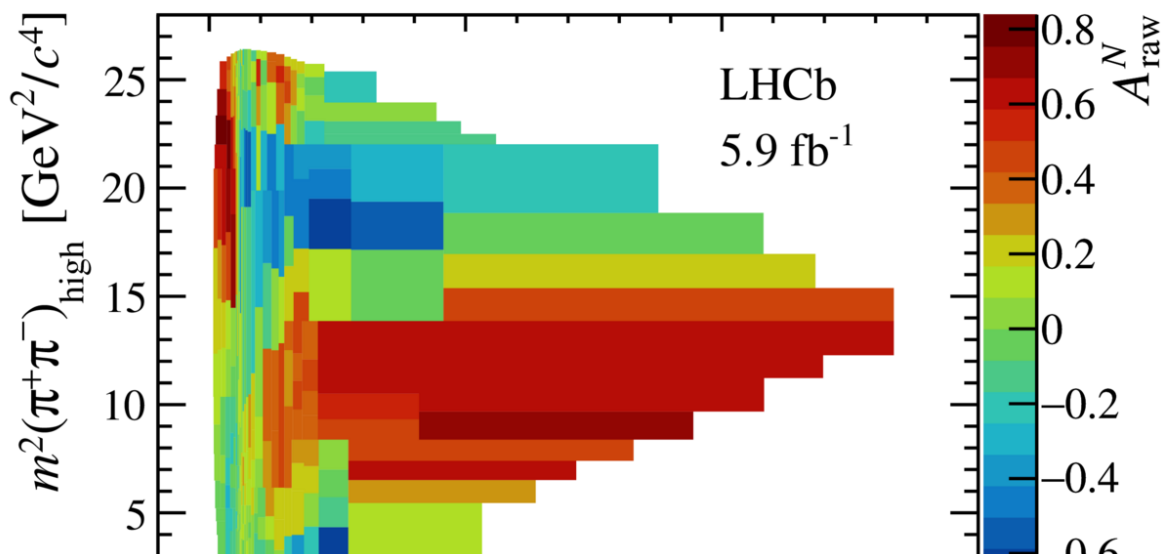
arXiv:2206.07622

Local asymmetries

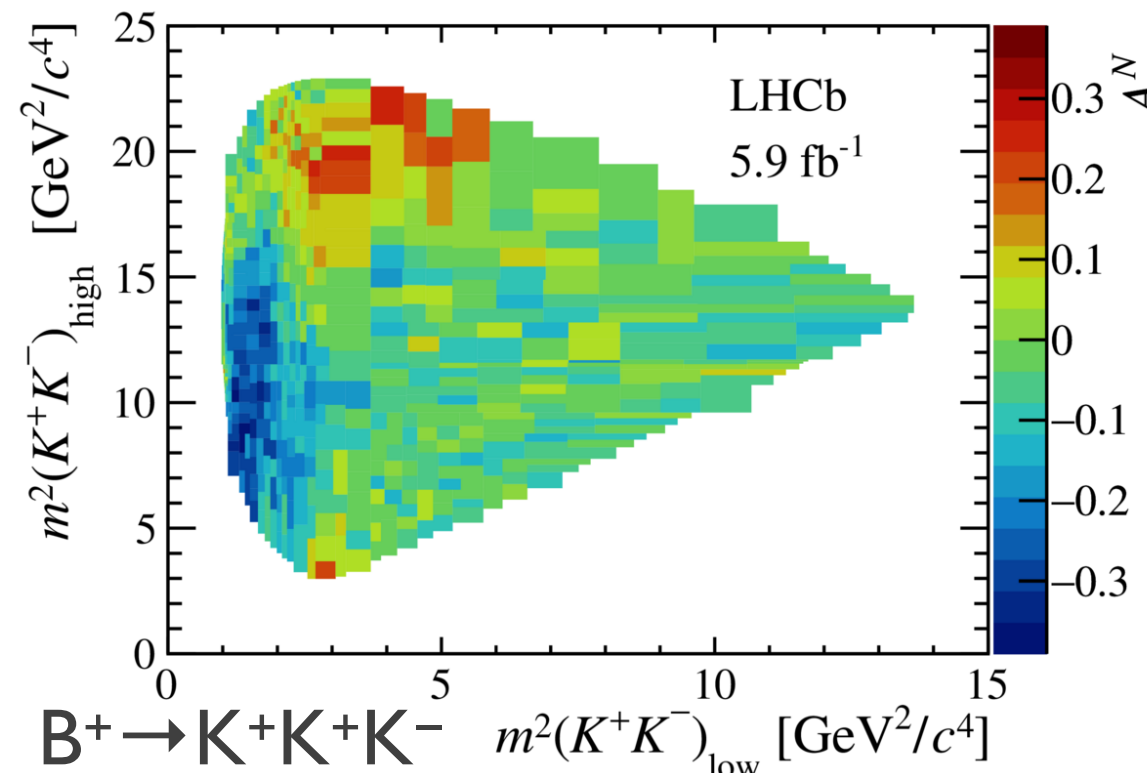
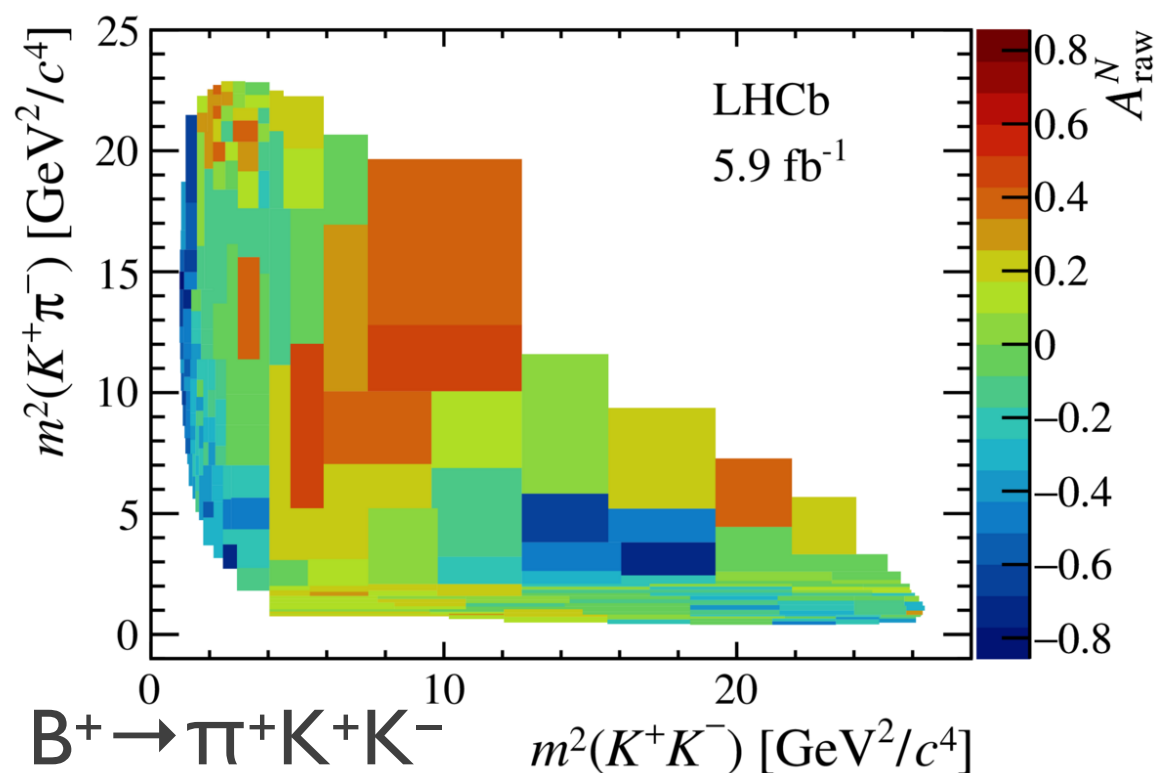


HEP
SCHEM

Local asymmetries



Suitable for computing lab for training undergrad students (with simplifications and small open data set from Run I)

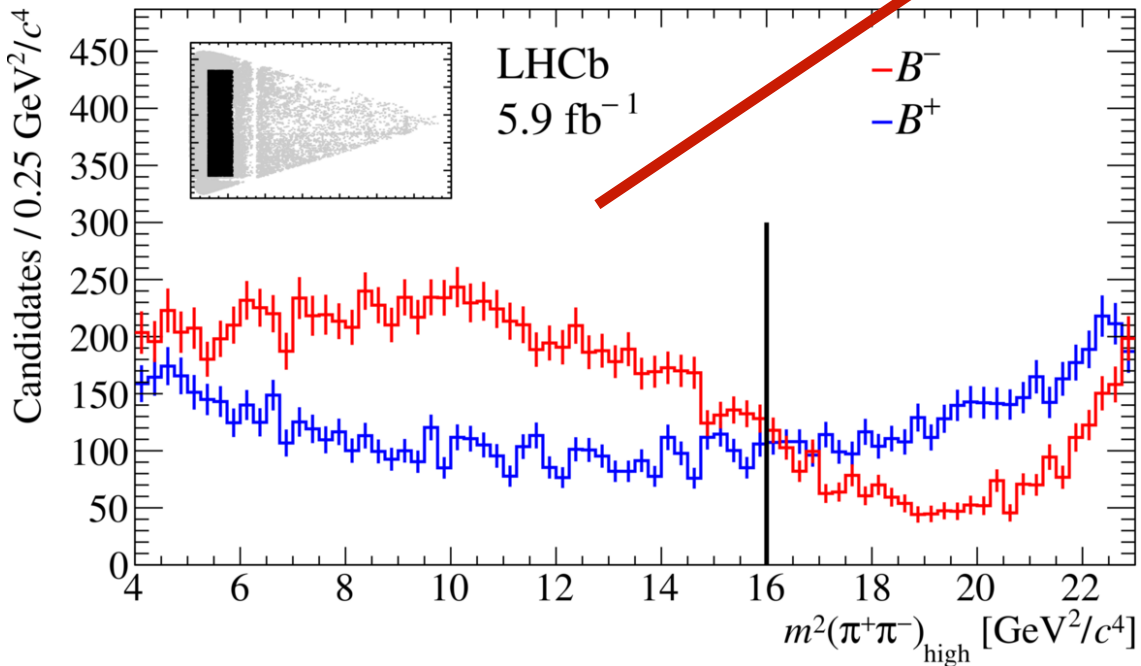


HEP
SCIENCE

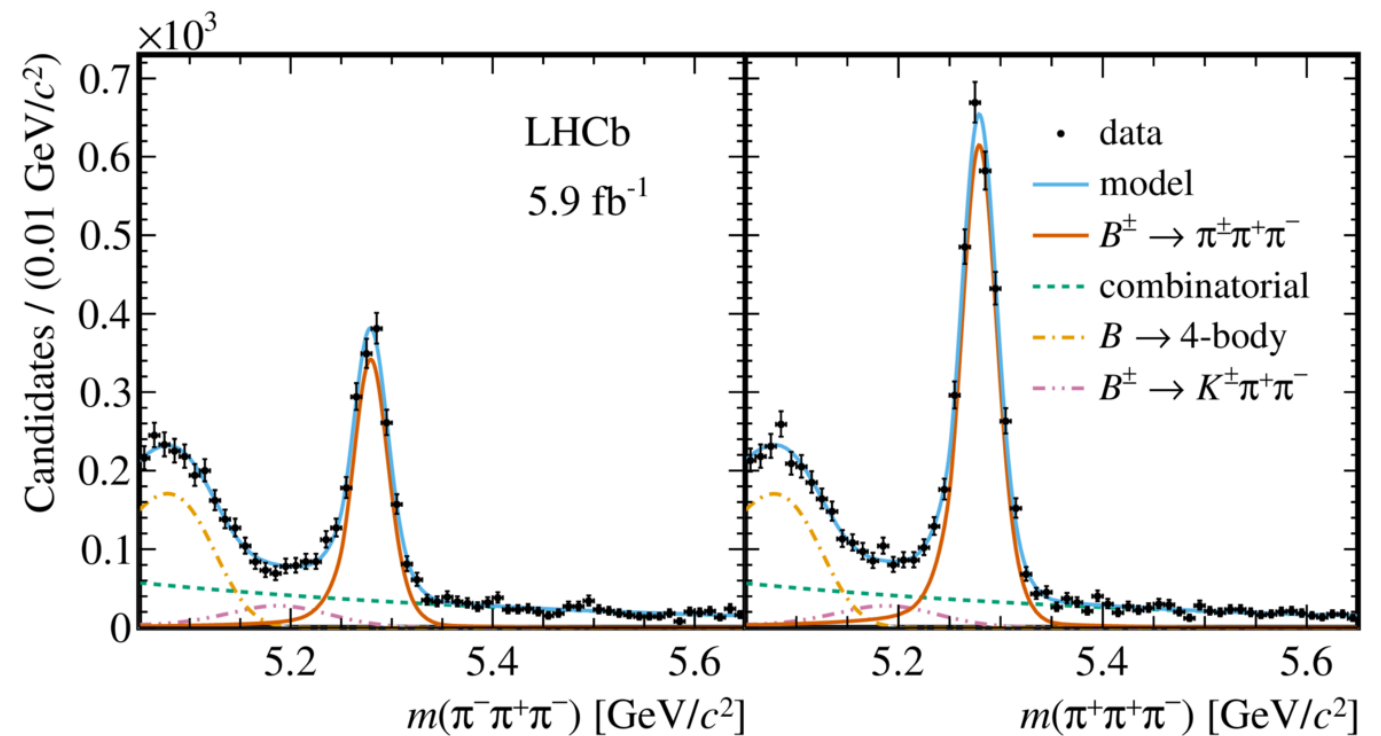
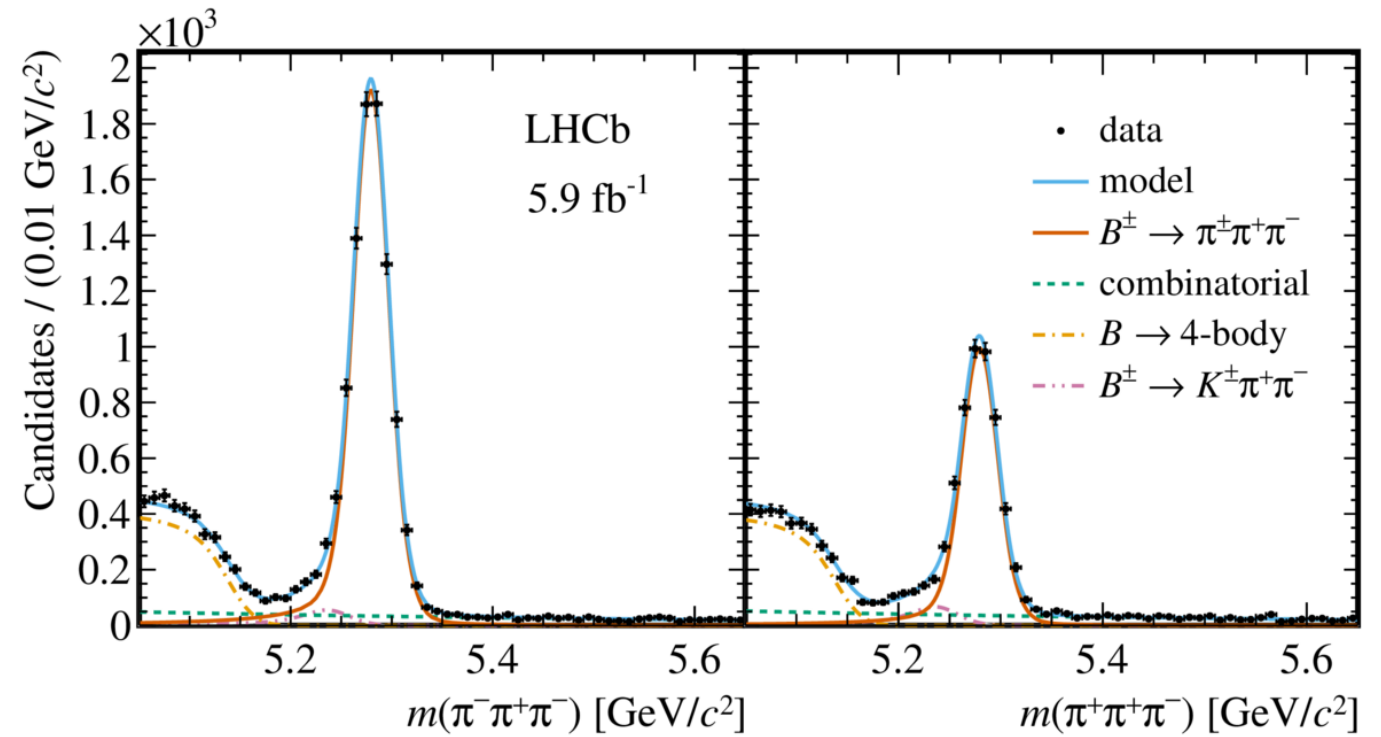
Local asymmetries and rescattering

- Rich pattern of large and localised asymmetries which result from interference between the contributions
- Possible $\pi\pi \rightarrow KK$ rescattering
- The rescattering region is defined in the Dalitz plot in the two-kaon or two-pion invariant mass range $1.1\text{--}2.25 \text{ GeV}^2/c^4$ for $B^+ \rightarrow K^+K^+K^-$ due to the presence of the $\phi(1020)$ resonance and $1\text{--}2.25 \text{ GeV}^2/c^4$ for the other three channels

Rescattering region $B^+ \rightarrow \pi^+\pi^+\pi^-$



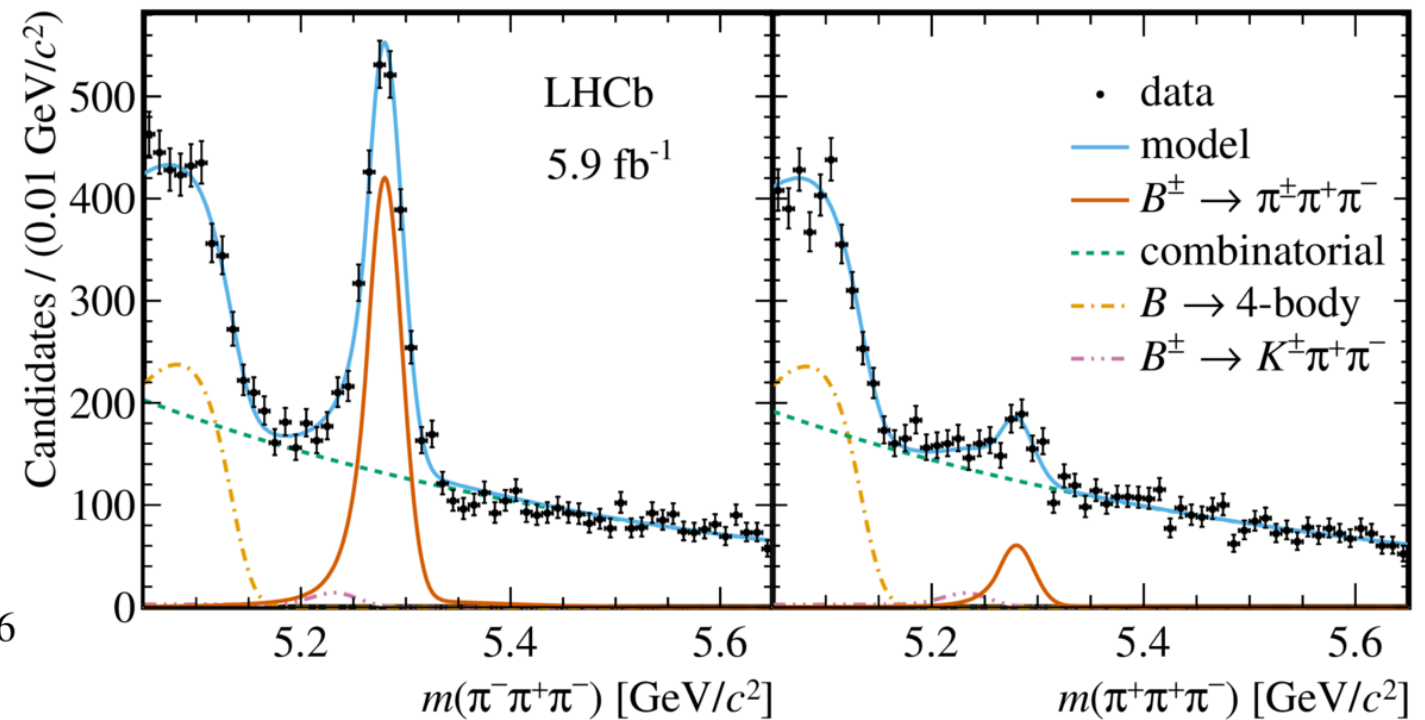
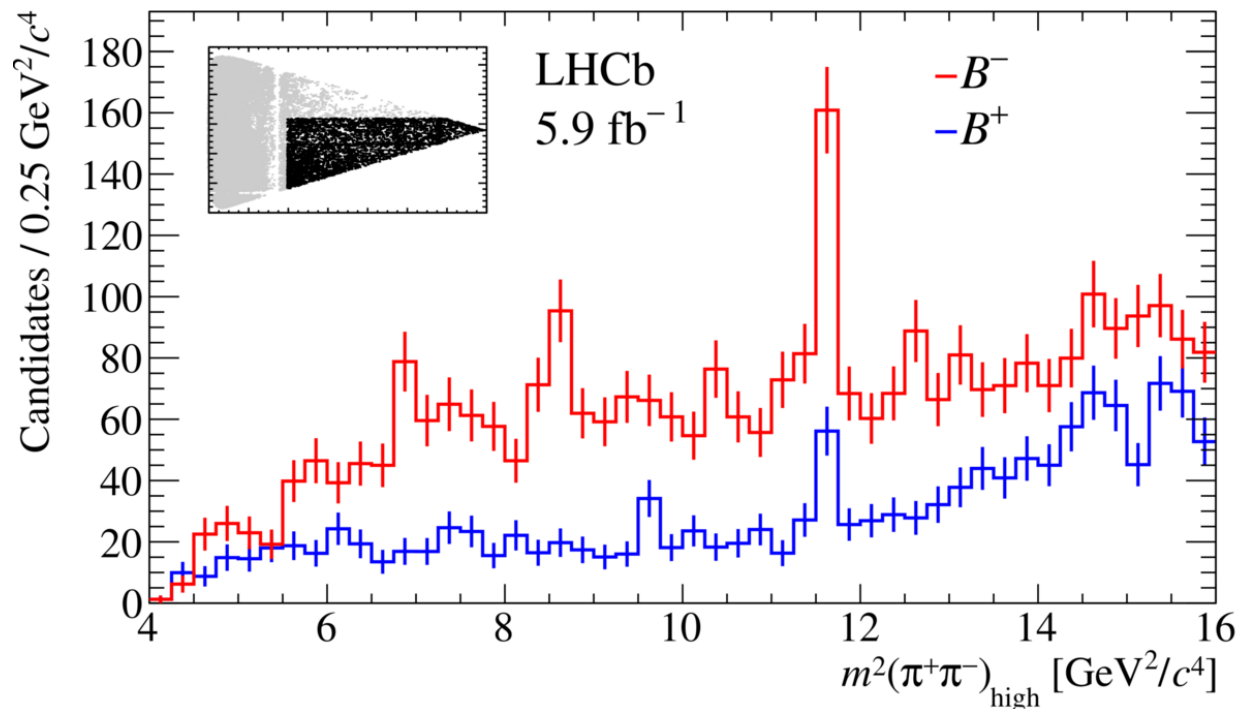
flip of the asymmetry
between the two regions



Higher mass region $B^+ \rightarrow \pi^+\pi^+\pi^-$



- Higher mass region
- Clear $\chi_{c0}(1P)$ contribution
 - comes from the B decay, as no such structure was observed in the invariant mass sidebands
- Large asymmetry is observed



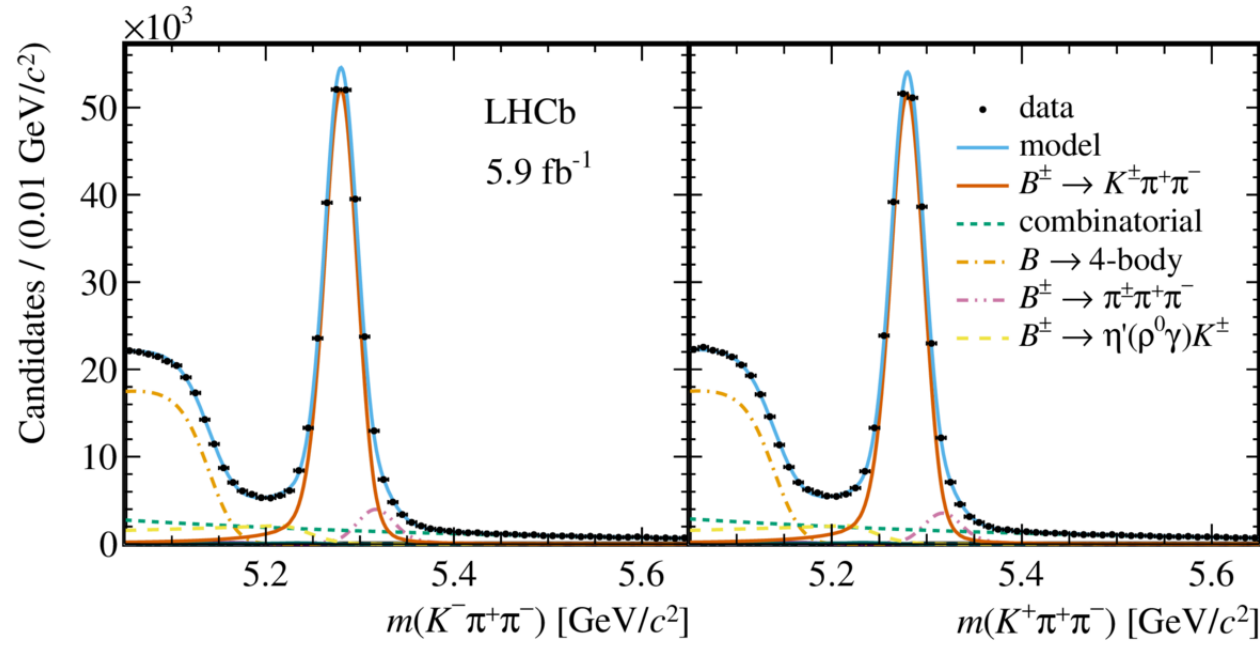
Integrated asymmetries

Direct CP violation in $B^\pm \rightarrow hhh$

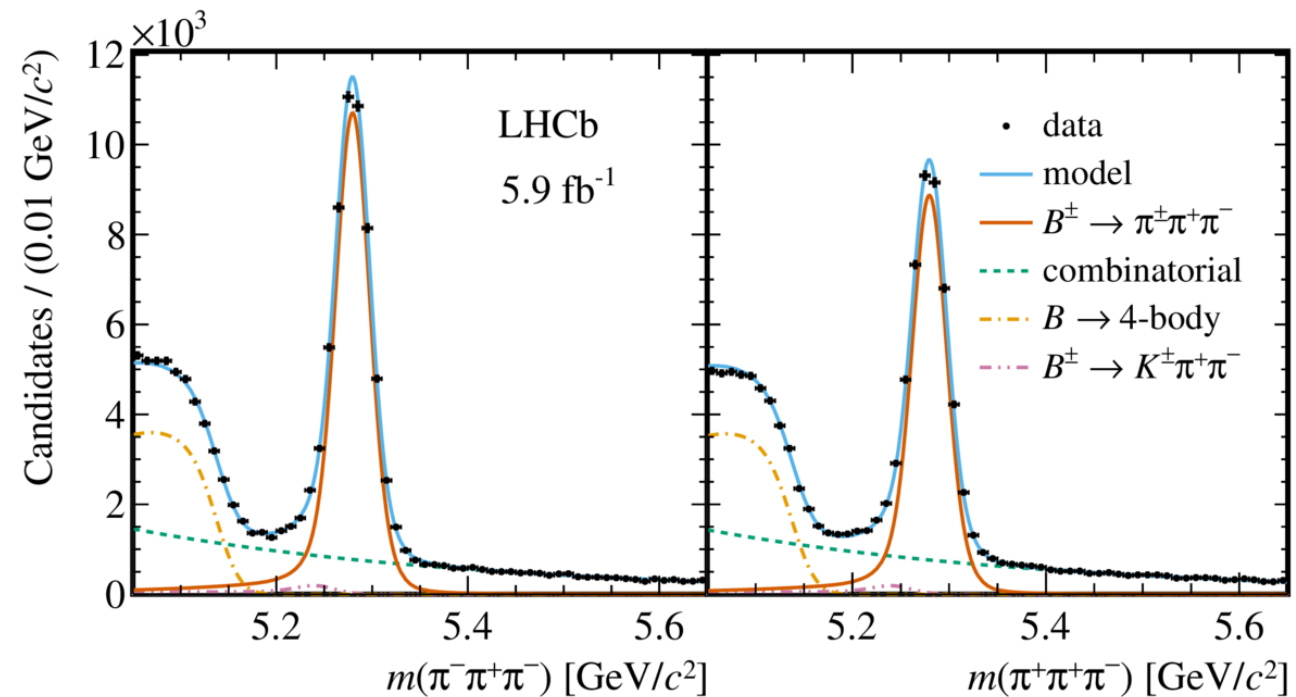
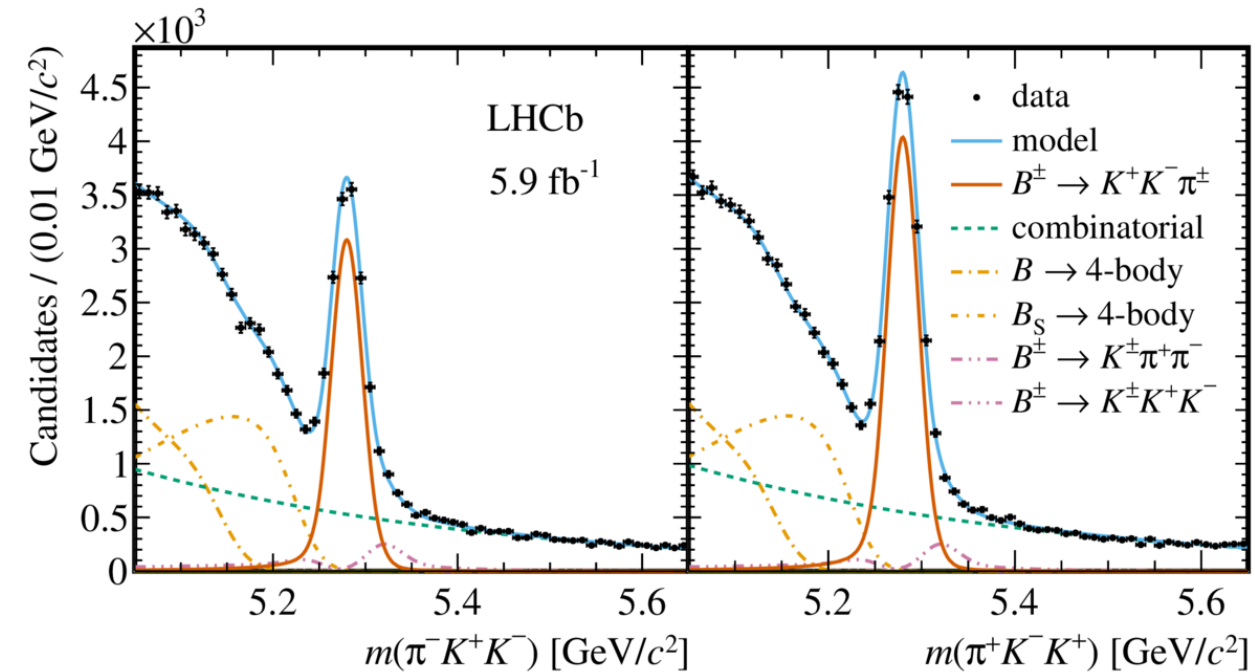
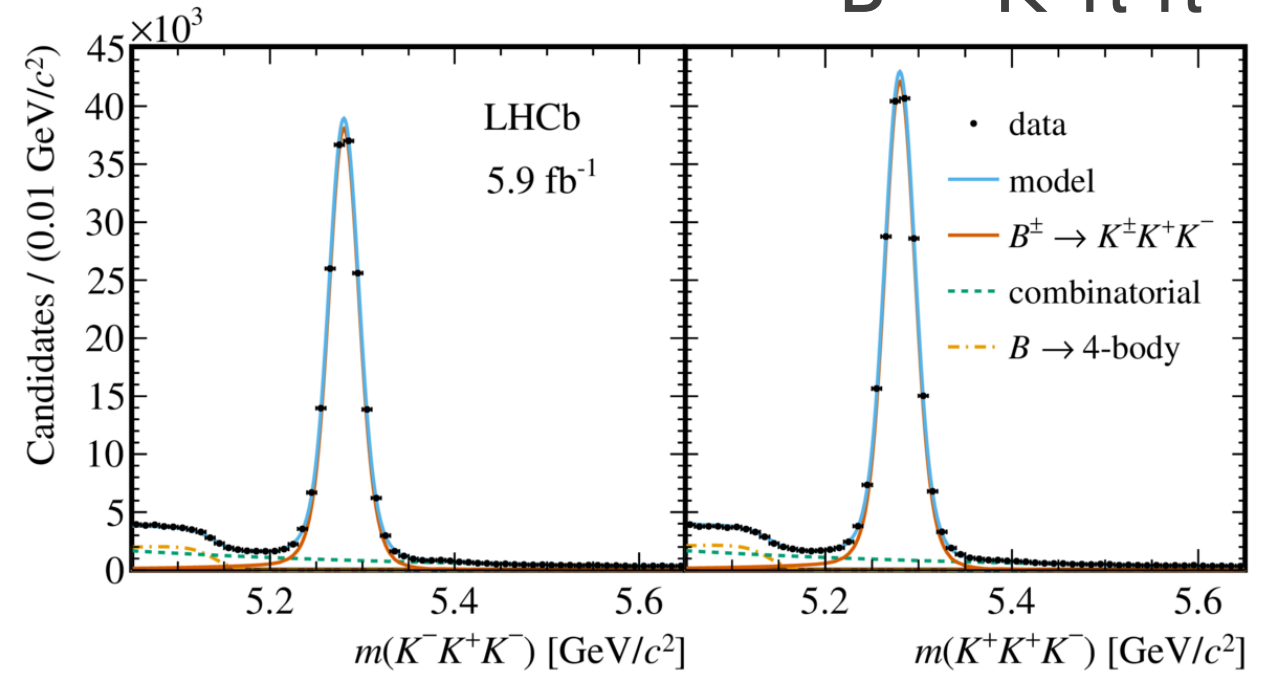
phase-space-integrated CP asymmetries

arXiv:2206.07622

$B^+ \rightarrow \pi^+ \pi^+ \pi^-$



$B^+ \rightarrow K^+ \pi^+ \pi^-$



$B^+ \rightarrow \pi^+ K^+ K^-$

$B^+ \rightarrow K^+ K^+ K^-$

- The CP asymmetry

$$A_{CP} = \frac{A_{raw}^{corr} - A_P}{1 - A_{raw}^{corr} A_P}$$

Production asymmetry

Efficiency corrected raw asymmetry

- Significant inclusive CP asymmetries are found for the latter three B decay channels, two observed for the first time

$$A_{CP}(B^{\pm} \rightarrow K^{\pm} \pi^{+} \pi^{-}) = +0.011 \pm 0.002 \pm 0.003 \pm 0.003,$$

$$A_{CP}(B^{\pm} \rightarrow K^{\pm} K^{+} K^{-}) = -0.037 \pm 0.002 \pm 0.002 \pm 0.003,$$

$$A_{CP}(B^{\pm} \rightarrow \pi^{\pm} \pi^{+} \pi^{-}) = +0.080 \pm 0.004 \pm 0.003 \pm 0.003,$$

$$A_{CP}(B^{\pm} \rightarrow \pi^{\pm} K^{+} K^{-}) = -0.114 \pm 0.007 \pm 0.003 \pm 0.003,$$

Also, results on U-spin asymmetries in arXiv:2206.07622

$B^\pm \rightarrow hhh$ and $B \rightarrow PV$

- The method that does not require full amplitude analyses
- The method is based on three key features of three-body B decays:
 - the large phase space
 - the dominance of scalar and vector resonances with masses below or around $1 \text{ GeV}/c^2$ (confirmed by amplitude analyses performed by Belle, BaBar and LHCb)
 - the clear signatures of the resonant amplitudes in the Dalitz plot
- Large phase space of these B-meson decays, different types of resonant contributions are allowed

The method for $B \rightarrow PV$

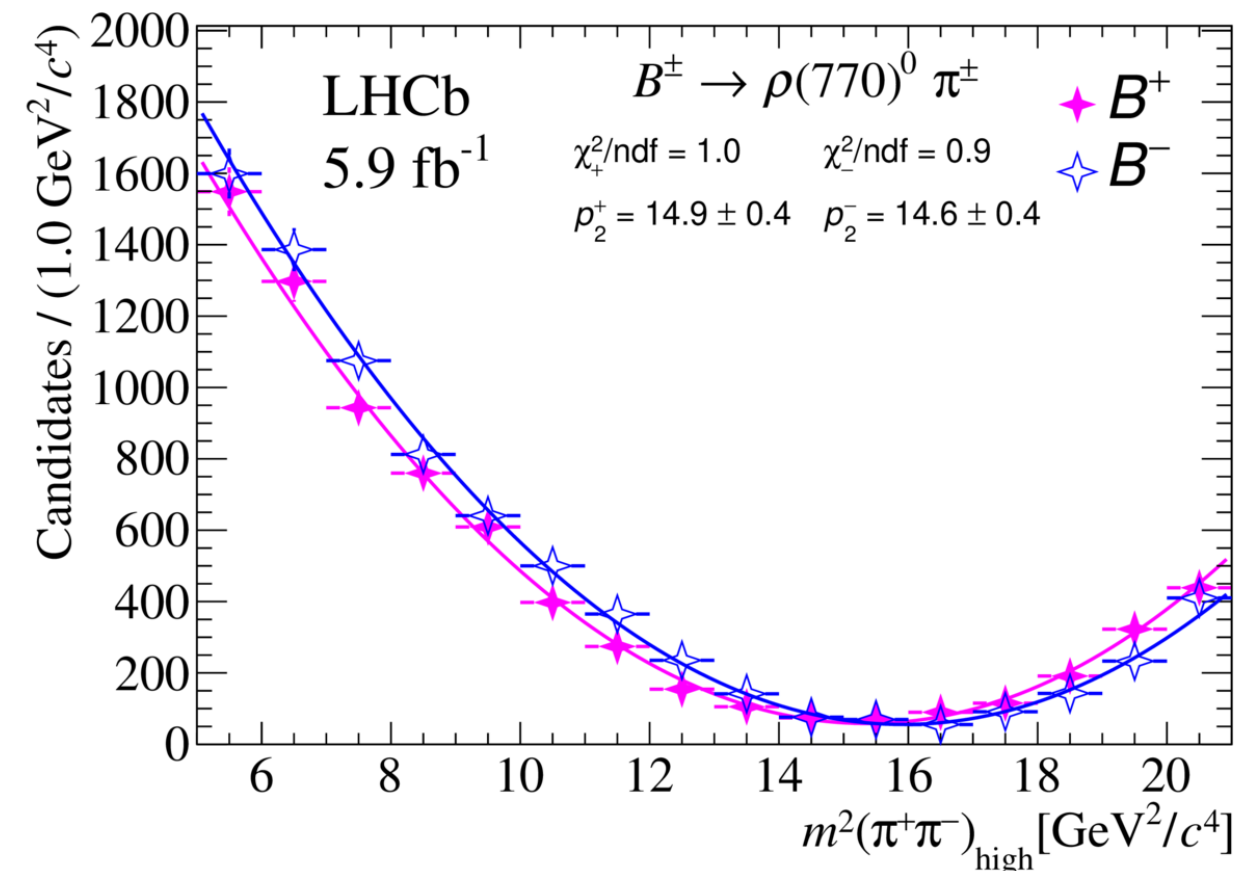
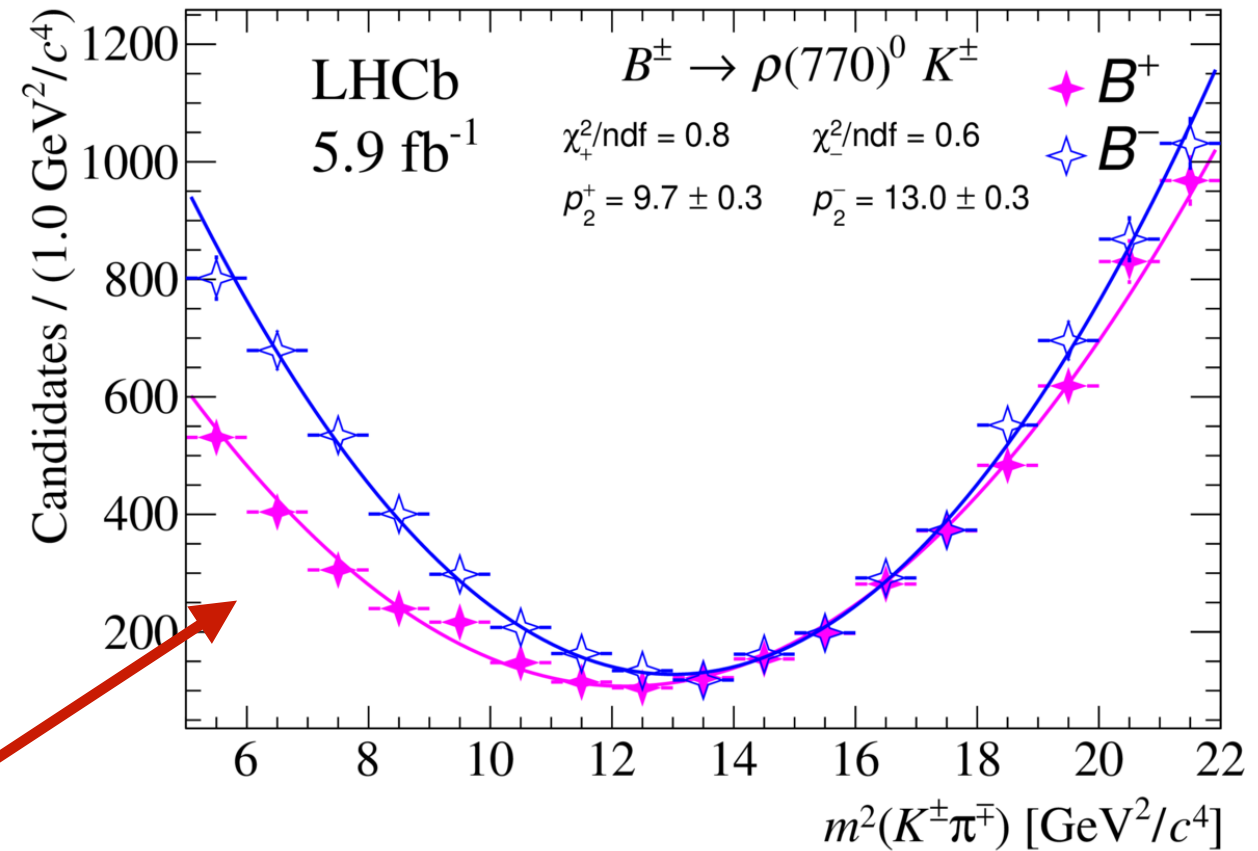
- Start with the decay $B^\pm \rightarrow R(\rightarrow h^-_1 h^+_2)h^\pm_3$:
 - R is an intermediate resonance
 - $s_{\parallel} = m^2(h^-_1 h^+_2)$ and $s_{\perp} = m^2(h^-_1 h^\pm_3)$
- The resonance line shape (typically a Breit-Wigner distribution) is observed in the projection of the Dalitz plot onto the s_{\parallel} axis
- When a narrow interval in s_{\parallel} around the resonance mass is selected, the projection of the data onto s_{\perp} reflects the angular distribution of the decay products.

The method for $B \rightarrow PV$ (continued)

arXiv:2206.02038

- Start with the decay $B^\pm \rightarrow R(\rightarrow h^{-1} h^{+2}) h^{\pm 3}$:
 - R is a intermediate resonance
 - $s_{\parallel} = m^2(h^{-1} h^{+2})$ and $s_{\perp} = m^2(h^{-1} h^{\pm 3})$
- **In vector resonances, a parabolic shape is observed**, since the decay width is proportional to cosine squared of the helicity angle, $\cos^2\theta$, where θ is defined as the angle between h^{-1} and $h^{\pm 3}$ computed in the $(h^{-1} h^{+2})$ rest frame.
- **If the $(h^{-1} h^{+2})$ pair forms a scalar resonance, the distribution in s_{\perp} is uniform**, since the decay of scalar resonances is isotropic in $\cos \theta$.

- Background components formed of these resonances plus a random track: has an angular distribution similar to the scalar resonances, so it is absorbed in the $p_{\pm 0}$ parameter.
- In the $\pi^+\pi^-$ P-wave, in the region dominated by the $B^\pm \rightarrow \rho(770)^0 K^\pm$
 $A_{CP} = +0.150 \pm 0.019 \pm 0.011$
- First observation of CP violation in this process
- Several other resonances tested:
 $B^\pm \rightarrow K^*(892)^0 \pi^\pm$, $B \rightarrow K^*(892)^0 K^\pm$ and $B^\pm \rightarrow \phi(1020) K^\pm$
 no other significant CP violation



MODEL DEPENDENT METHODS

Dalitz plot analysis features

- Interference plays a significant role in the phase space distributions and in the physics sensitivity
- Amplitude analysis can explore several features of multibody decays
 - Relative phases between states
 - Sensitivity to CP violating effects
 - Resolve ambiguities in weak phases
 - Hadron spectroscopy

Amplitude analysis

- Amplitude: sum of contributions

$$\mathcal{A}(m_{12}^2, m_{23}^2) = \sum_{j=1}^N A_j(m_{12}^2, m_{23}^2) = \sum_{j=1}^N c_j F_j(m_{12}^2, m_{23}^2)$$

c_i : complex coefficients describing the relative magnitude and phase of the different isobars

F_i : dynamical amplitudes that contain the lineshape and spin-dependence of the hadronic part

Resonance mass term
(e.g. Breit–Wigner)

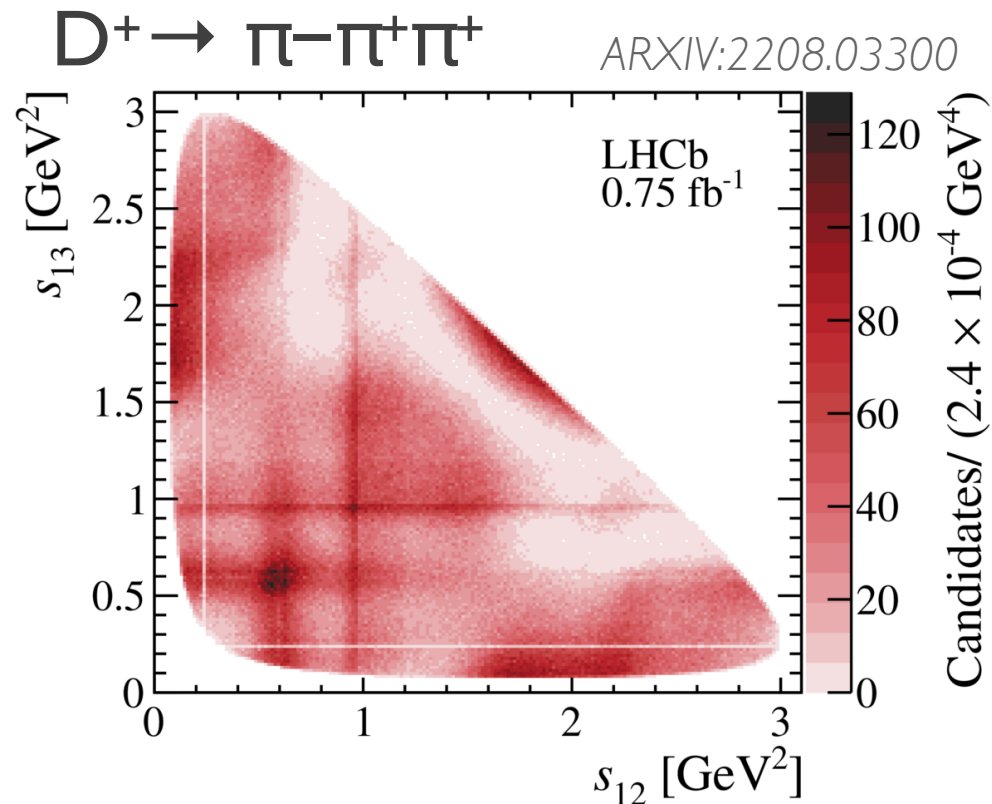
Barrier factors - p, q : momenta
of bachelor and resonance

Angular probability
distribution

- S-wave (non-resonant component) description difficult, increasingly turning to multiple approaches
- Isobar: Each contribution has clear physical meaning
- K-matrix: Experimental interface scattering results that enforce 2-body unitarity
- Quasi-model-independent: Binned amplitude determined directly from data

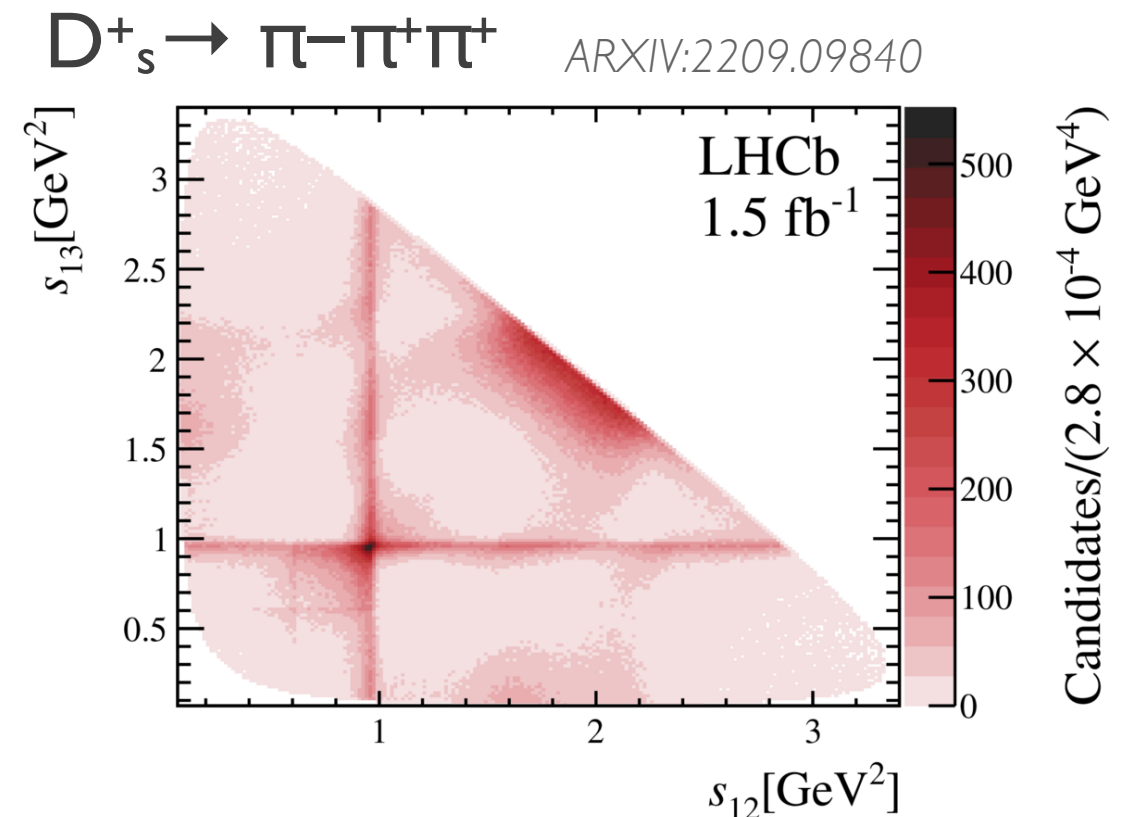
S-wave dominant for $D^+_{(s)} \rightarrow \pi^- \pi^+ \pi^+$

Quasi-model-independent partial-wave analysis, in which the $\pi^+ \pi^-$ S-wave amplitude is parameterised as a generic complex function determined by a fit to the data.



The S-wave component dominant, followed by the $\rho(770)^0 \pi^+$ and $f_2(1270) \pi^+$ components.

First observation of the $\omega(782) \rightarrow \pi^- \pi^+$ decay



The S-wave dominant, followed by the contribution from spin-2 resonances and a small contribution from spin-1 resonances.

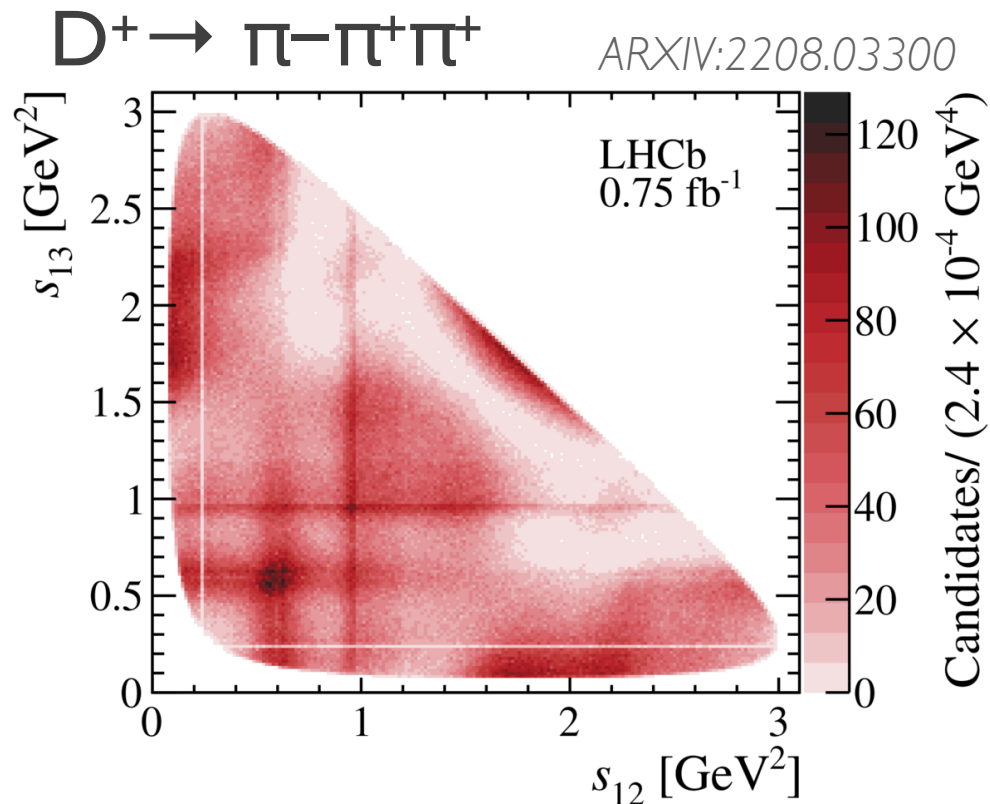
First observation of the $D^+_s \rightarrow \omega(782) \pi^+$ channel in the $D^+_s \rightarrow \pi^- \pi^+ \pi^+$ decay.

S-wave dominant for $D^+(s) \rightarrow \pi^- \pi^+ \pi^+$

Quasi-mode
is parameter

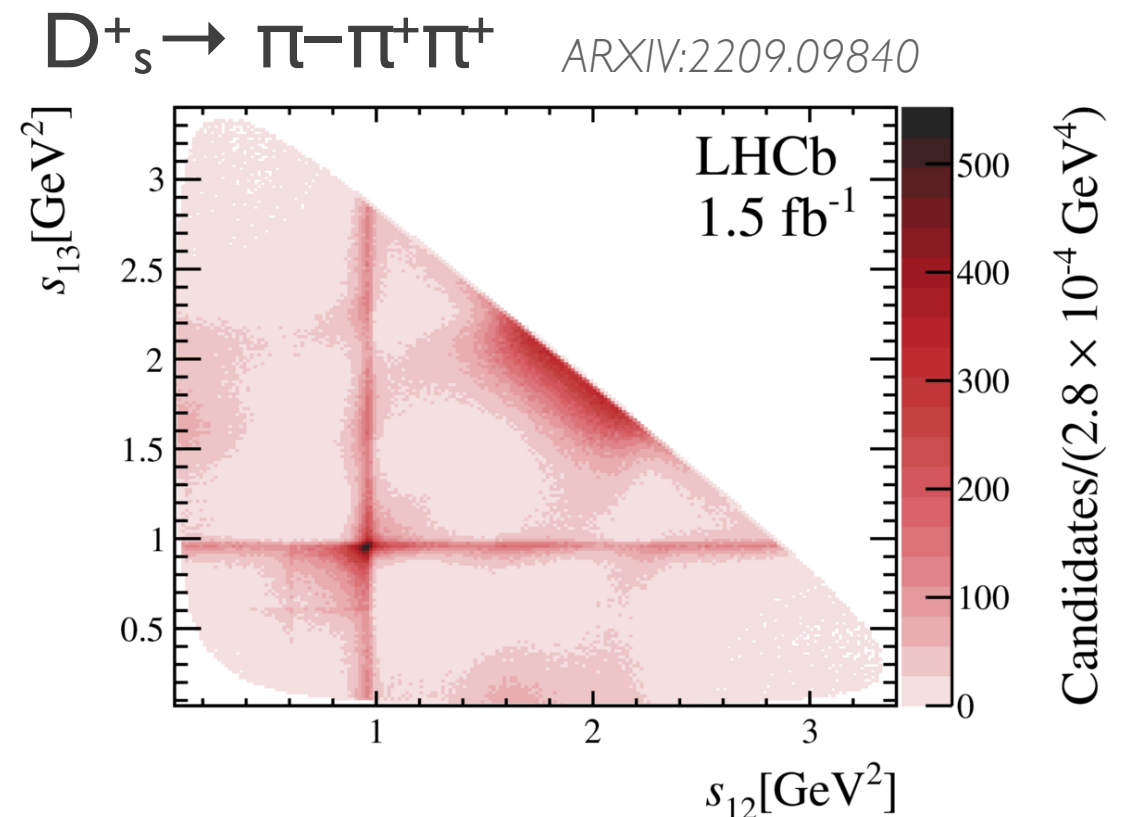
$$\mathcal{A}(s_{12}, s_{13}) \equiv \mathcal{A}_S(s_{12}, s_{13}) + \sum_i a_i e^{i\delta_i} \mathcal{A}_i(s_{12}, s_{13}) + (s_{12} \leftrightarrow s_{13})$$

wave amplitude
it to the data.



The S-wave component dominant, followed by the $\rho(770)^0 \pi^+$ and $f_2(1270) \pi^+$ components.

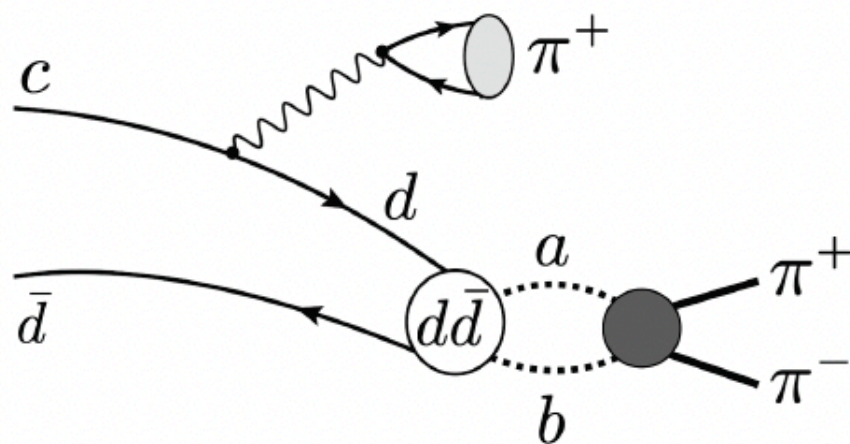
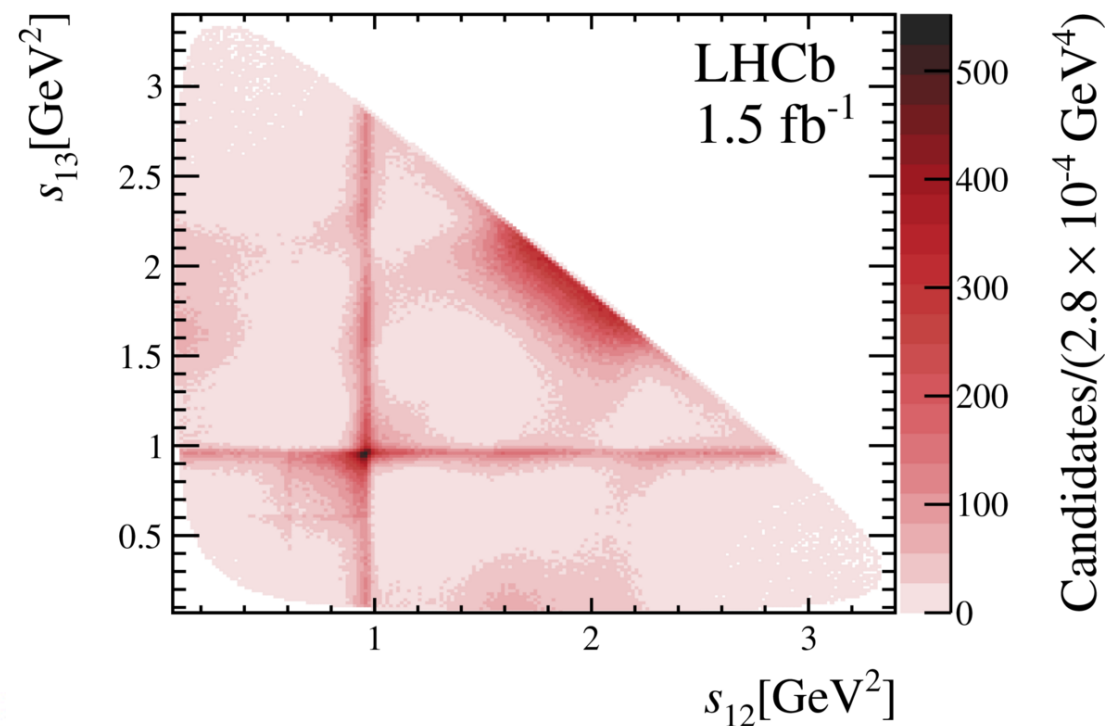
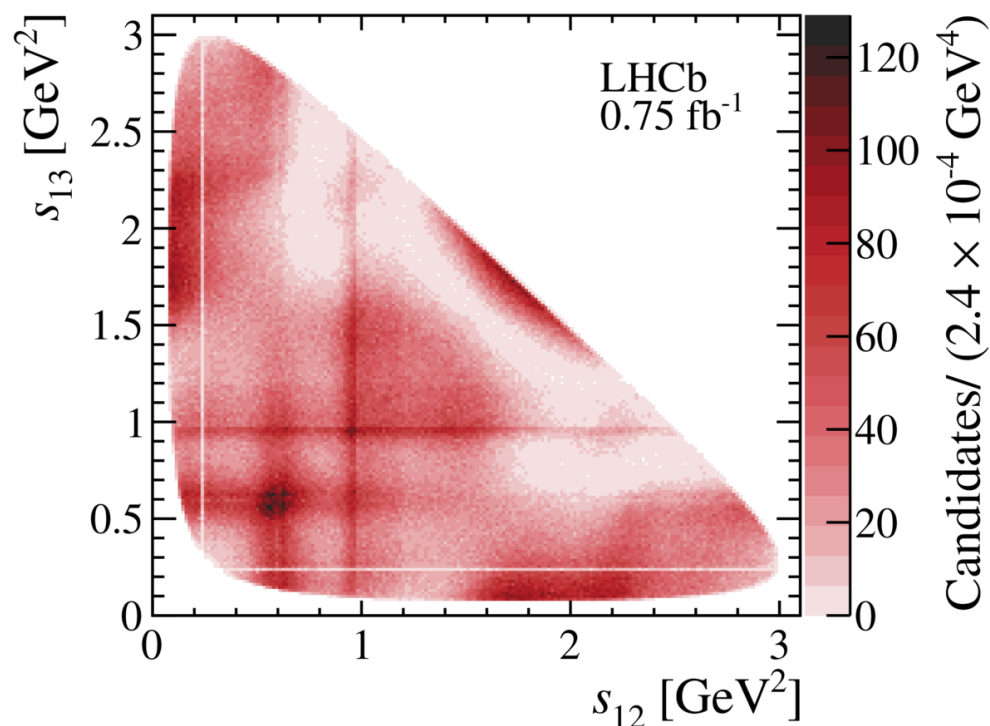
First observation of the $\omega(782) \rightarrow \pi^- \pi^+$ decay



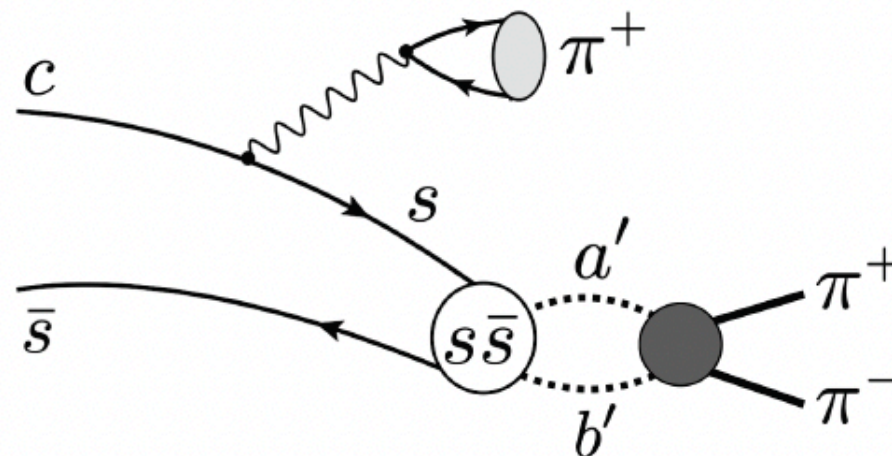
The S-wave dominant, followed by the contribution from spin-2 resonances and a small contribution from spin-1 resonances.

First observation of the $D_s^+ \rightarrow \omega(782) \pi^+$ channel in the $D_s^+ \rightarrow \pi^- \pi^+ \pi^+$ decay.

S-wave comparison

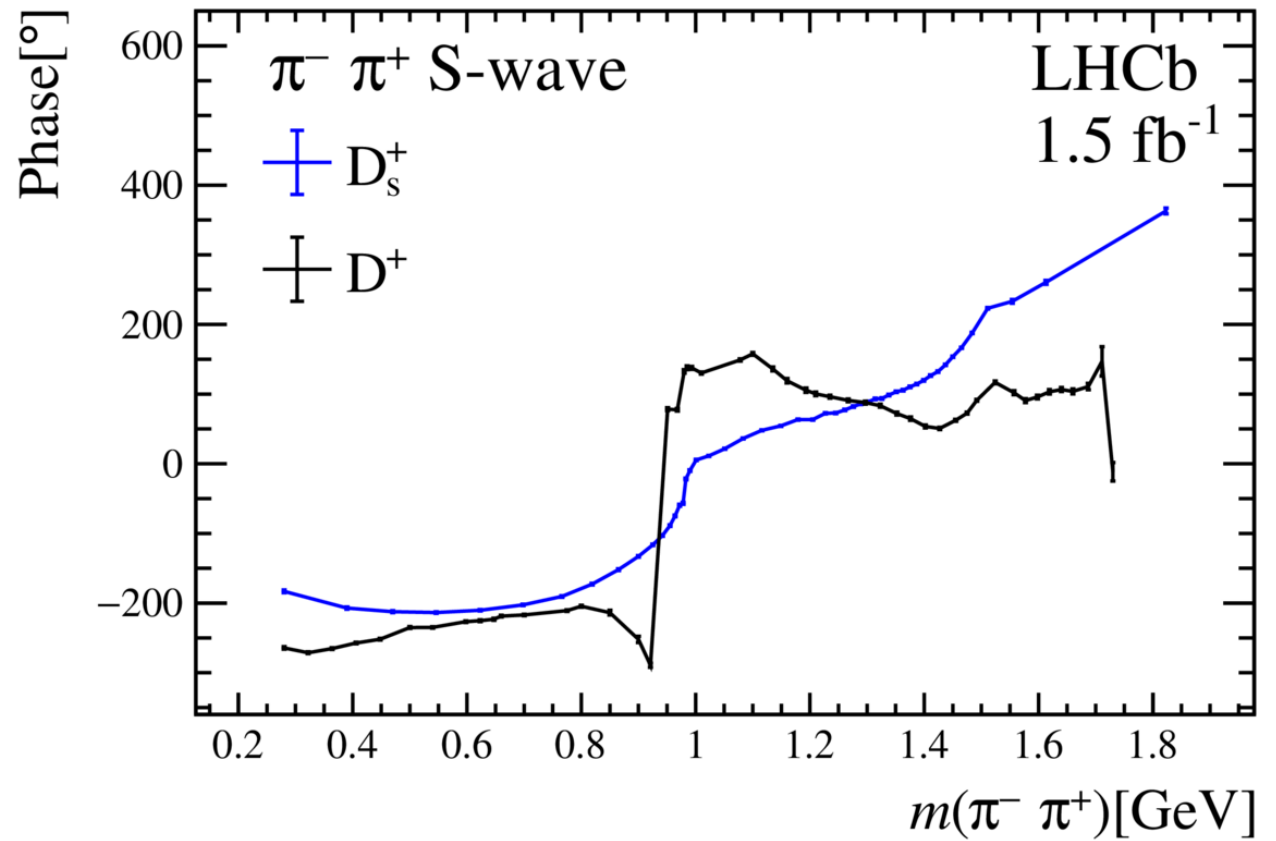
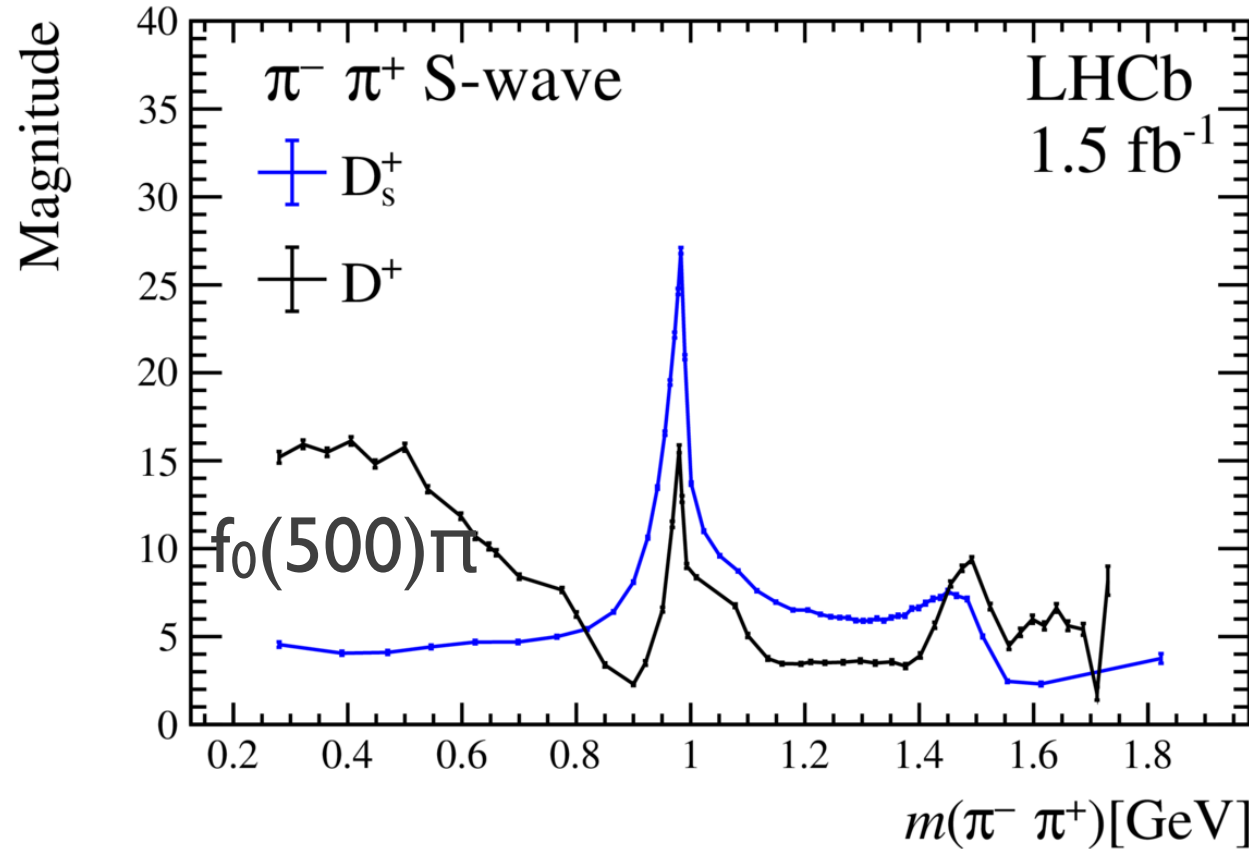


S-wave formed by the reactions $ab \rightarrow \pi\pi\pi$, such as $\pi^+\pi^-, \pi^0\pi^0, \pi^0\eta, K^0\bar{K}^0$



S-wave formed by the reactions $ab \rightarrow \pi\pi\pi$, with $s(\bar{u}u + \bar{d}d + \bar{s}s)$ such as $K^+K^-, K^0\bar{K}^0, \eta\eta$

S-wave comparison



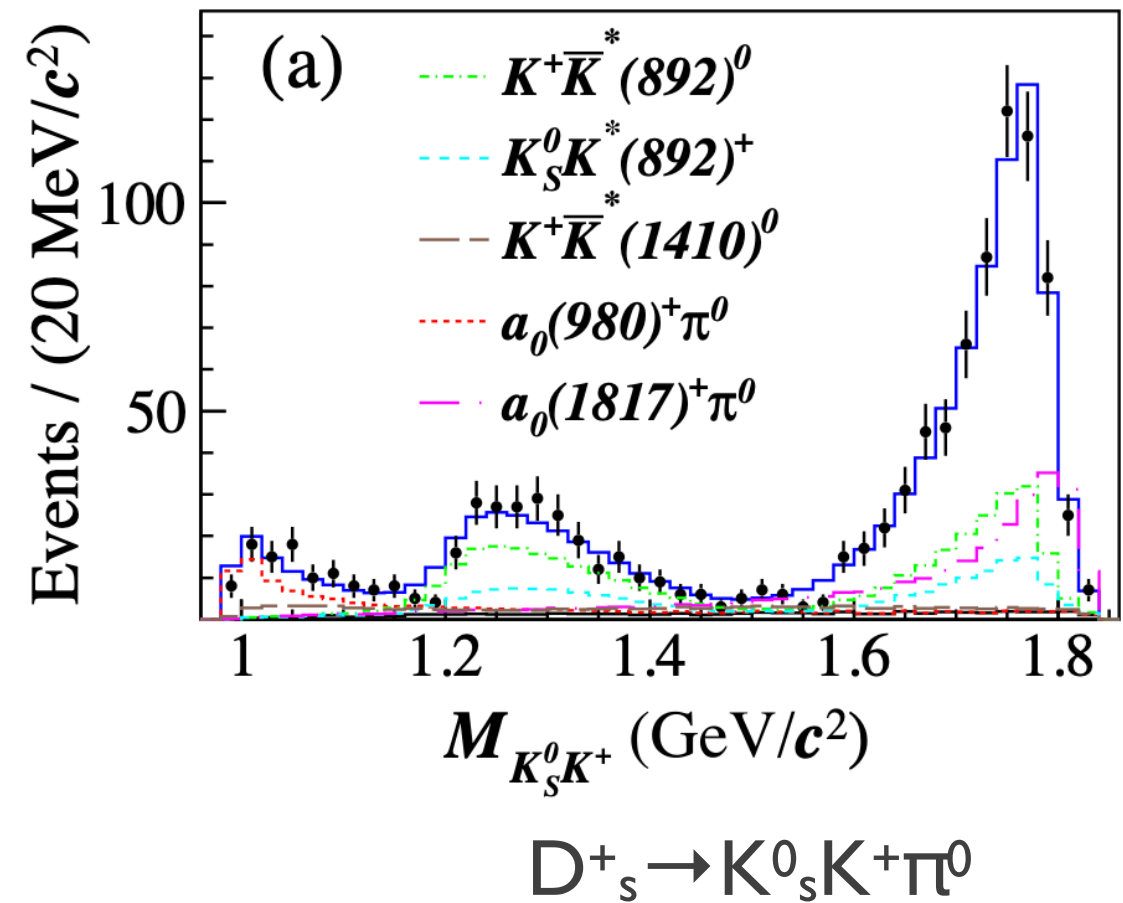
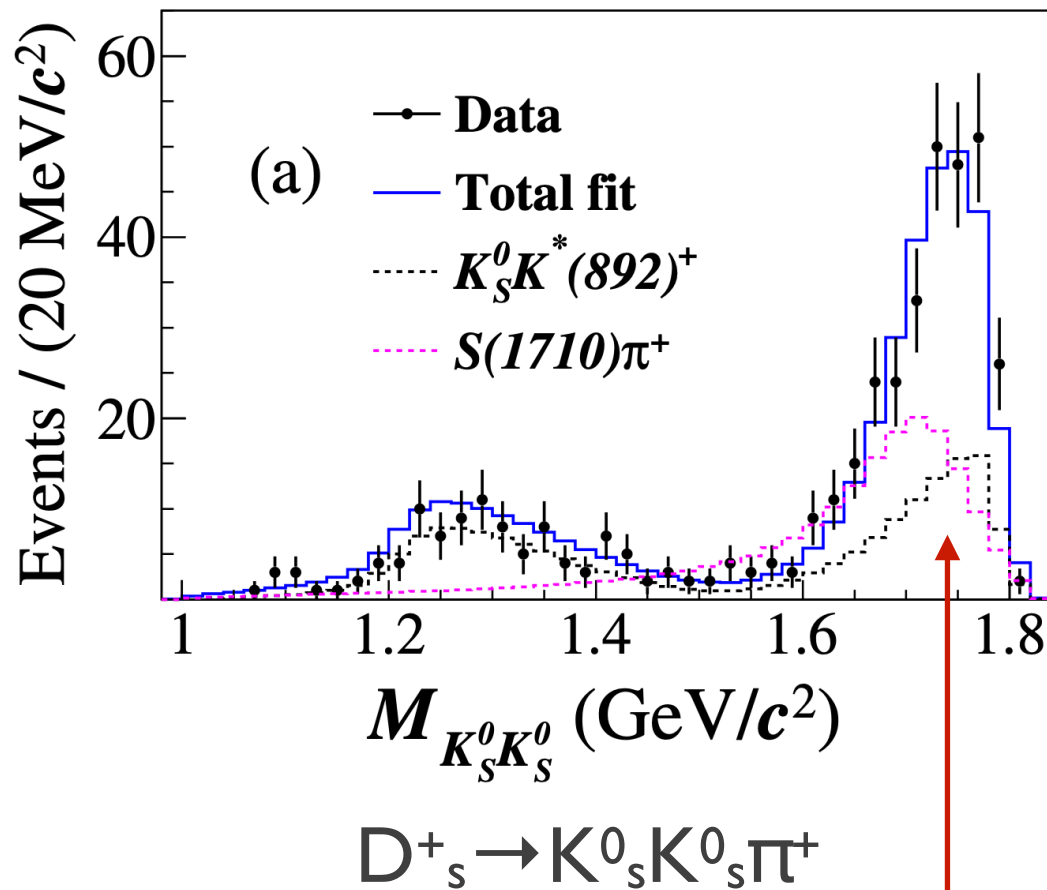
$f_0(980)\pi$: couples strongly to KK

mode	$D_s^+ \rightarrow \pi^- \pi^+ \pi^+$	$D^+ \rightarrow \pi^- \pi^+ \pi^+$
S-wave	84.97 ± 0.14	61.82 ± 0.5
P-wave	8.55 ± 0.44	32.31 ± 0.64
D-wave	13.12 ± 0.02	13.8 ± 0.2

First amplitude analysis of $D_s^+ \rightarrow K_s^0 K_s^0 \pi^+$

PHYS. REV. D 105, L051103 (2022)

PRL 129(2022)182001

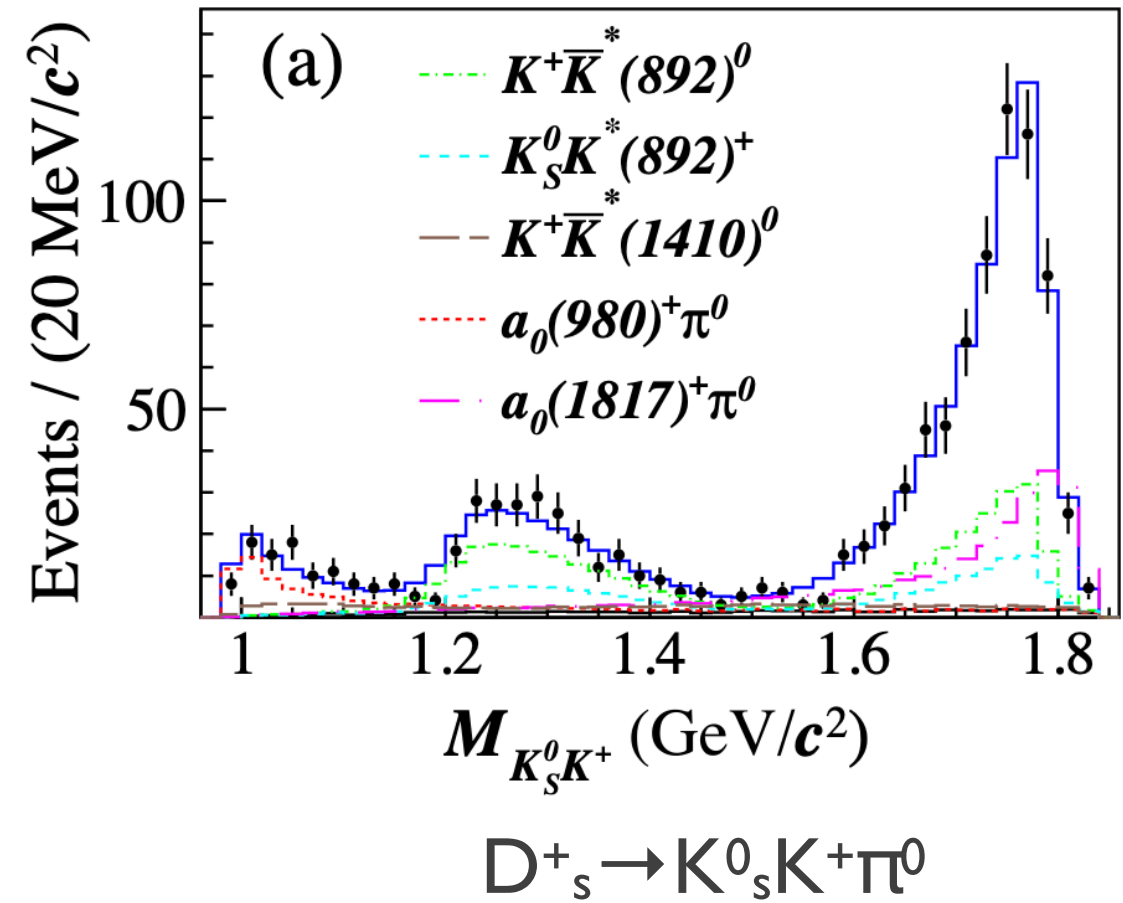
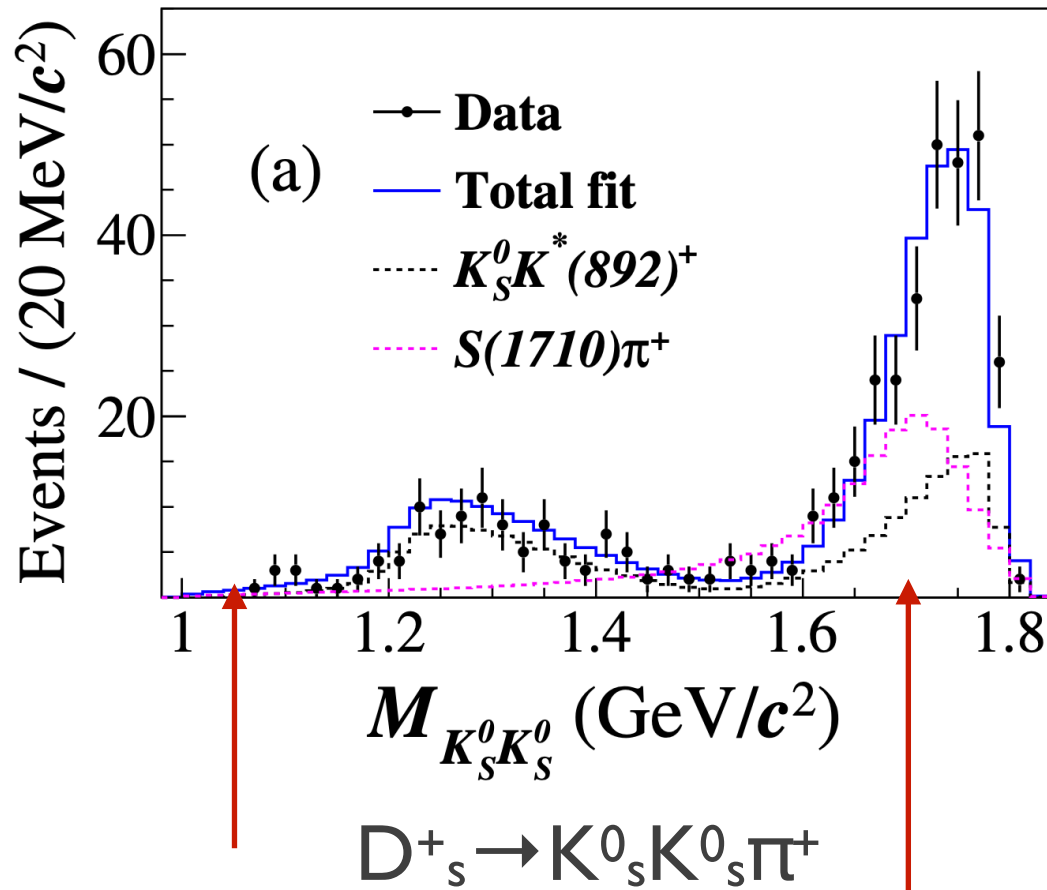


- 6.32 fb^{-1} collected at COM energies between 4.178 and 4.226 GeV
- Enhancement in $K_S^0 K_S^0$ and $K_S^0 K^+$ near $1.7 \text{ GeV}/c^2$: isospin one partner of the $f_0(1710)$?
- Same resonance observed by BaBar in $\eta c \rightarrow \pi \pi \eta$?

First amplitude analysis of $D_s^+ \rightarrow K_s^0 K \pi$

PHYS. REV. D 105, L051103 (2022)

PRL 129(2022)182001



destructive interference between $a_0(980)^0$ and $f_0(980)$

implies the existence of an isospin one partner of the $f_0(1710)$ meson, the $a_0(1710)^0$: supports KK^* molecule

hypothesis rather than a glue ball

$$M = 1.817 \pm 0.008 \pm 0.020 \text{ GeV}/c^2,$$

$$\Gamma = 0.097 \pm 0.022 \pm 0.015 \text{ GeV}/c^2$$

$$\mathcal{B}(D_s^+ \rightarrow a_0(1817)^+ \pi^0) = (3.44 \pm 0.52 \pm 0.32) \times 10^{-3} \quad \text{Significance} > 10\sigma$$

Loads of amplitude analyses

[Amplitude analysis and branching fraction measurement of the decay \$D^+ \rightarrow K_S^0 \pi^+ \pi^0 \pi^0\$](#)
2305.15879

[Amplitude analysis of \$D^0 \rightarrow K_L^0 \pi^+ \pi^-\$](#)
2212.09048

[Amplitude analysis and branching fraction measurement of \$D_s^+ \rightarrow K^+ \pi^+ \pi^- \pi^0\$](#)
2205.13759

[Amplitude Analysis and Branching Fraction Measurement of \$D_s^+ \rightarrow K^+ \pi^+ \pi^-\$](#)
2205.08844

[Amplitude Analysis and Branching Fraction Measurement of \$D_s^+\$ to \$K_S^0 K^+ \pi^0\$](#)
2204.09614

[Amplitude Analysis and Branching Fraction Measurement of \$D_s\$ to \$K^+ K^- \pi^+ \pi^- \pi^0\$](#)
2203.06688

[Amplitude Analysis and Branching Fraction Measurement of \$D_s^+ \rightarrow \pi^+ \pi^0 \eta\$](#)
2202.04232

[Amplitude Analysis and Branching Fraction Measurement of \$D_s^+\$ to \$K_S^0 K_S^0 \pi^+\$](#)
2110.07650

[Amplitude Analysis and Branching Fraction Measurement of \$D_s^+ \rightarrow \pi^+ \pi^0 \pi^0\$](#)
2109.12660

[Dalitz-plot analysis of \$D^+ \rightarrow \pi^+ \pi^- \pi^+\$](#)
2108.10050

[Amplitude analysis and branching fraction measurement of \$D_s^+ \rightarrow \eta \pi^+ \pi^- \pi^0\$](#)
2106.13536

[Amplitude analysis of the decay \$D^+ \rightarrow K^+ K_S^0 \pi^0\$](#)
2104.09131

[Amplitude Analysis and Branching Fraction Measurement of \$D_s^+ \rightarrow K_S^0 \pi^+ \pi^0\$](#)
2103.15098

[Amplitude Analysis and Branching Fraction Measurement of \$D_s^+ \rightarrow K^- K^+ \pi^+ \pi^0\$](#)
2103.02482

[Amplitude Analysis and Branching Fraction Measurement of \$D_s^+ \rightarrow K^- K^+ \pi^+ \pi^0\$](#)
2103.02482

[Amplitude Analysis and Branching Fraction Measurement of \$D_s \rightarrow K^+ K^- \pi^+\$](#)
2011.08041

[Amplitude Analysis and BF measurement of \$D^0 \rightarrow K^- \pi^+ 2\pi^0\$](#)
1903.06316

[Amplitude analysis of \$D_s^+ \rightarrow \pi^+ \pi^0 \eta\$](#)
1903.04118

[Amplitude analysis of \$D^+ \rightarrow K_S^0 \pi^+ \pi^+ \pi^-\$](#)
1901.05936

[Amplitude analysis of \$D^0\$ to \$K^- \pi^+ \pi^+ \pi^-\$](#)
1701.08591

BESIII: PRD 95 (2017) 7, 072010

Dalitz analysis of $D^0 \rightarrow K^- \pi^+ \eta$ decays at Belle

Belle Collaboration, published in [PRD 102, 012002 \(2020 July 6\)](#)

D to $4h^{(\prime)}$ decays : LHCb: JHEP 02 (2019) 126

LHCb: Eur. Phys. J. C78 (2018) 443

CLEO-c data: JHEP 05 (2017)



Summary

- Unique sensitivity to CP violation
- Important for QCP tests
- A plethora of methods to explore multibody decays
- Development of model unbiased methods is an interesting challenge
- Many interesting results, very active field